

REPORT DOCUMENTATION PAGE

AFRL-SR-BL-TR-98-

Public reporting burden for this collection of information is estimated to average 1 hour per response, including the time for reviewing instructions, searching existing data sources, gathering the required data, reviewing the collection of information, Send comments regarding this burden estimate or any other aspect of this collection of information, including suggestions for reducing the burden, to Washington Headquarters Services, Directorate for Information Operations and Reports, 1215 Jefferson Davis Highway, Suite 1204, Arlington, VA 22202-4302, and to the Office of Management and Budget, Paperwork Project (0142-0047).

ig and reviewing
for Information

1. AGENCY USE ONLY (Leave blank)	2. REPORT DATE 9 JAN 98	3. REPORT TYPE AND DATES COVERED FINAL REPORT 1 SEP 93 - 31 AUG 97
4. TITLE AND SUBTITLE (AASERT-FY93) WIND TUNNEL "FREE FLIGHT" ON A DYNAMIC STRUT		5. FUNDING NUMBERS F49620-93-1-0455 3484/WS 61103D
6. AUTHOR(S) D. P. TELIONIS		
7. PERFORMING ORGANIZATION NAME(S) AND ADDRESS(ES) VIRGINIA POLYTECHNIC INSTITUTE AND STATE UNIVERSITY ENGINEERING SCIENCE AND MECHANICS DEPARTMENT BLACKSBURG, VA 24061-0219		8. PERFORMING ORGANIZATION REPORT NUMBER
9. SPONSORING/MONITORING AGENCY NAME(S) AND ADDRESS(ES) AIR FORCE OFFICE OF SCIENTIFIC RESEARCH (AFOSR) 110 DUNCAN AVENUE SUITE B115 BOLLING AFB DC 20332-8050 NA		10. SPONSORING/MONITORING AGENCY REPORT NUMBER

19980129 063

12a. DISTRIBUTION STATEMENT (If the distribution statement is "unlimited", the distribution code is "U".)	12b. DISTRIBUTION CODE
unlimited	

13. ABSTRACT (Maximum 200 words)

Work on this project was distributed to various tasks. The first was design construction and calibration of a simple, one-degree-of-freedom model. the second was the development of fuzzy-logic software needed to control the motion. The third was appropriate balance systems and dynamic calibration techniques. A roll moment balance system was designed and constructed. The system was mounted to a stepper motor via a shaft which played the role of a roll actuator. The electronic components and software necessary to provide direct feedback were constructed and tested. A computer program was written and tested. As input to the program we employed the reading of pressure transducers connected with a seven-hole probe. The desired output was the actual orientation of the probe as well as the static and dynamic pressure. The program was employed to generate static pressure, dynamic pressure and three-components of the velocity in terms of the signals obtained by the pressure transducers. To further test this software it was decided to employ a dynamic mechanism which is available and operational. This involved the response of a ship hull to oncoming waves. The fuzzy logic system was trained with data obtained with different wave characteristics and ship incidences. The idea was to train the artificial intelligence system to predict the response of the vessel, namely pitch and roll characteristics to new conditions. More specifically, the ship "learns" to recognize the condition of the sea it finds itself in. It then predicts how it will response, if it points in a different direction.

14. SUBJECT TERMS

DEMO CONCEPT INTEGRATED 2

15. NUMBER OF PAGES

53

16. PRICE CODE

17. SECURITY CLASSIFICATION
OF REPORT

UNCLASSIFIED

18. SECURITY CLASSIFICATION
OF THIS PAGE

UNCLASSIFIED

19. SECURITY CLASSIFICATION
OF ABSTRACT

UNCLASSIFIED

20. LIMITATION OF
ABSTRACT

30 DEC 1997

FINAL REPORT
ON
WIND TUNNEL "FREE FLIGHT" ON A DYNAMIC STRUT

ASSERT-AFOSR No. F49620-93-1-0455

prepared by

D. P. Telionis
Engineering Science and Mechanics
Virginia Polytechnic Institute and State University
Blacksburg, VA 24061-0219

November 1997

Abstract

Work on this project was distributed to various tasks. The first was design construction and calibration of a simple, one-degree-of-freedom model. The second was the development of fuzzy-logic software needed to control the motion. The third was appropriate balance systems and dynamic calibration techniques.

1. One-and two-degree of freedom simulators

A roll moment balance system was designed and constructed. The system was mounted to a stepper motor via a shaft which played the role of a roll actuator. The electronic components and software necessary to provide direct feedback were constructed and tested.

At the end of the balance, a bar was mounted and connected with springs to demonstrate the simulation of harmonic motions. The system then was operated as follows. The bar was displaced from its equilibrium position and then was released. The couple exerted by the springs was detected by the balance system and was fed to the computer. The computer then integrated the differential equation of the motion by a small time step, for a prescribed artificial moment of inertia and determined the corresponding angular rotation $\Delta\phi$. It then activated the roll actuator to perform a rotation $\Delta\phi$. The process was repeated and thus harmonic motions were executed.

The package was debugged and a delta wing model has been mounted on the sting. The plan is to employ this mechanism in order to simulate wing rock in the wind tunnel. The advantage of this approach is that then the moment of inertia of the model will be entered as a parameter of the software. Combined motions were tested subsequently. To this end the software was prepared which allows the operation of the three-degrees-of-freedom dynamic strut described in the proposal. This simulation is described in Appendix I. This was the senior project of Mr. Tomlin, one of the undergraduate students who worked on this project.

A second generation roll moment balance system was then designed and constructed. The system was mounted to a stepper motor via a shaft which played the role of a roll actuator. The electronic components and software necessary to provide direct feedback were constructed and tested. A schematic of the drive hardware can be seen in Fig. 1. The system bulk has been reduced from this initial design by the use of smaller bearing houses, fewer bearings, and a smaller motor.

A second generation load cell has also been constructed using a very thin (0.005") aluminum tube. The new load cell greatly exceeds the sensitivity of earlier designs but still maintains sufficient structural strength to withstand the dynamic loads which it must transmit from the model to the sting. Sensitivity was further increased by the mounting of two parallel, high resistance strain gauge bridges on the cell.

Because of the small forces being measured in this experiment, amplification is necessary to achieve a useful output from the system. Still, the system has been plagued by electromagnetic noise which adversely affects the closed loop control of the model by introducing no-load instability. A great deal of effort has gone into the solution of this problem and noise has been reduced to an acceptable level.

A method to accurately calibrate the load cell was also developed. The calibration scheme incorporates a fuzzy logic system so that the calibration can be adapted to any changes in system response due to changes in mechanical or environmental states. Unfortunately, this

phase of the work has not yet been completed.

Development of a pneumatically driven "mini-DyPPiR" is underway. This system will allow for three-degree-of-freedom dynamic control of the model and would again employ an adaptive fuzzy logic control system. If successful, the mini-DyPPiR would be superior to the current stepper-motor driven rotational system, because it would offer smooth rotation at low speeds. Because of the nature of stepper-motors, the high sensitivity load cell picks up vibrations from the motor at low stepping rates.

2. Fuzzy Logic Controller

It is anticipated that complex feedback loops will be necessary to control model motions in the wind tunnel. It is believed that the prediction of such motions and their controls can be achieved more efficiently with fuzzy logic techniques.

A computer program was written and tested. As input to the program we employed the reading of pressure transducers connected with a seven-hole probe. The desired output was the actual orientation of the probe as well as the static and dynamic pressure. The program was employed to generate static pressure, dynamic pressure and three-components of the velocity in terms of the signals obtained by the pressure transducers.

As a first step, the code was employed for system identification in high-alpha delta-wing unsteady aerodynamics. A delta wing, equipped with cavity flaps or an apex flap, was tested executing pitch-up maneuvers while the flaps are dynamically employed, aiming to modify and control the behavior of the two leading-edge vortical structures and thus their effect on the pressure distribution and aerodynamic loading of the wing. The fuzzy identifier was constructed to predict the temporal evolution of the leeward pressure distribution and the aerodynamic loads for given time histories of pitching, $\alpha(t)$, $\dot{\alpha}(t)$, and flap deployment $\phi(t)$, $\dot{\phi}(t)$. Work on this topic is described in greater detail in Appendix II.

The fuzzy logic system used in this experiment is based on an optimized system as outlined by Wang¹ for identifying non-linear systems in control applications. The program

which was used has been under development with the goal of eventually controlling systems whose aerodynamic/hydrodynamic effects are too complex to model for classical control purposes. In its early stages of development, the program has been used successfully to fit complex curves based on partial data sets. It accepts as input the following data: A cluster radius for determining the complexity of the fuzzy rule base, a Gaussian membership function shape variable which determines the effect of a fuzzy rule on its surroundings, and the training input-output pairs.

The cluster radius determines the minimum amount that one point in the training data must differ from all other points in order to be part of a new fuzzy rule. The advantage of this clustering method is that for any given system and cluster radius, there is a limit to the number of fuzzy rules which can be created. Thus the cluster radius directly determines the complexity of the fuzzy rule base for any given system. Here, the cluster radius was chosen so that each input-output pair created a new rule, thereby ensuring that the program would return accurate values at the original data points.

The Gaussian membership function shape variable has by far the most significant effect on the smoothing effect of the predictor program and therefore the most care must be taken in its specification^{1,2}. If the shape variable is too small, then all predicted values will take on the magnitude of the nearest fuzzy rule, resulting in large regions of like points. If, on the other hand, the shape variable is chosen too large, then a fuzzy rule will affect a large area of surrounding values, possibly including other rule supports or center values. This will result in very smooth but inaccurate results. It is, therefore, imperative that a reasonable compromise be determined between these conditions. For the purposes of this experiment, this compromise was found through trial and error, although it seems likely that with a thorough knowledge of the input-output ranges and the cluster radius, a more rigorous method of determining this value should be possible.

To further test this software it was decided to employ a dynamic mechanism which is

available and operational. This involved the response of a ship hull to oncoming waves. The fuzzy logic system was trained with data obtained with different wave characteristics and ship incidences. The idea was to train the artificial intelligence system to predict the response of the vessel, namely pitch and roll characteristics to new conditions. More specifically, the ship "learns" to recognize the condition of the sea it finds itself in. It then predicts how it will response, if it points in a different direction.

The data taken for this experiment consisted of 13 angles of incidence ranging from -30° to 30° in 5° increments. The incident waves were generated at three different magnitudes at 0.25 Hz and 0.5 Hz for a total of 78 different data sets. Each data set in turn contained time records of two water level transducers separated by 21", the roll angle of the ship and the pitch angle of the ship. Each time record was 10 seconds long and was sampled at 100 Hz. Unfortunately, it was determined after the data had been taken that the largest magnitude wave at 0.5 Hz was affected by some sort of mechanical interference and thus had to be removed from the training set.

To test the code, a case for intermediate values of the parameters was predicted. At these values of the parameters data were also obtained which were not employed in the training of the fuzzy-logic system. In this way it was possible to compare directly the predicted behavior against experimental data.

Typical results are presented in Figs. 2 and 3 for roll and pitch respectively, for an incidence of 15° at a wave frequency of 0.5 Hz. The phase and frequency of the response of the model are predicted reasonably well. However, the waveform contains higher harmonics which are not present in the actual data.

This work was presented at an ASME meeting and is described in greater detail in Appendix III. The method was subsequently applied to predict pressure distributions over a delta wing controlled by deployable surfaces. This was presented at an AIAA conference. The paper is attached as Appendix IV. The latest development on this project will be presented

at the AIAA annual meeting in January 1998. A first draft of this paper is attached as Appendix V.

References

1. Wang, Li-Xin, "Adaptive Fuzzy Systems and Control, Design and Stability Analysis," Prentice Hall, New Jersey, 1994.
2. Kosko, Bart, "Neural Networks and Fuzzy Systems," Prentice Hall, New Jersey, 1992.
3. Husson, D., "The Design of the Charles-de-Gaulle," Carenas, April 1955.
4. Student Performance

Two undergraduate students have worked on this project. Mr. Tim Tomlin developed and tested the first simulator. He was later accepted in the graduate school but decided to work on another project. Mr. Christopher Moore, a graduate student, has carried out most of the work on this project. His efforts were somewhat hampered by the fact that the mother project, namely the main project which this AASERT was supposed to complement was not renewed. Mr. Moore earned a Masters degree and continued for a while his efforts but then unfortunately for the progress on this effort and perhaps fortunately, for him, he decided to get married and accepted a lucrative offer from industry. Due to lack of funds, it was not possible to use the Dynamic Strut in the VPI Stability Tunnel which this group has helped design and construct. It was thus decided to develop an alternative simulator. This was the project of another student, Mr. Joon Pak, who is an undergraduate student. Mr. Pak has transferred from electrical engineering and continues working with this team. Finally, Mr. Schaeffler, a Ph.D. student, has contributed to this project. Mr. Schaeffler will defend his Ph.D. dissertation in December 1997.

5. Publications

The following publications have resulted from this project and are attached as Appendices to this final report.

1. "A smart Oscillator Which Simulates Harmonic Motion," Timothy Tomlin, VPI & SU Senior Project, May 1994.
2. "Fuzzy Logic and Neural Network System Identification for High-Alpha Delta Wing Maneuvers with Deployable Control Surfaces," by Furey, D. A., Rediniotis, O. K., Moore, C. T., Schaeffler, N. W., and D. P. Telionis, AIAA Paper No. 96-0894, June 1996.
3. "Fuzzy Logic Identification of Ship Motions in Response to Varying Wave Incidence," by C. T. Moore, and D. P. Telionis, ASME FED Vol. 242, pp. 35-38, Nov 1996.
4. "A Fuzzy Controller for High-Alpha Delta Wing Maneuvers with Deployable Control Surfaces," by Rediniotis, O. K., Schaeffler, N. W., and D. P. Telionis, AIAA Paper No. 96-0894, January 1996.
5. "Dynamic Delta Wing Pitch-Up Control Via Apex Flaps," by N. W. Schaeffler and D. P. Telionis, AIAA Paper No. 98-0637, January 1998.

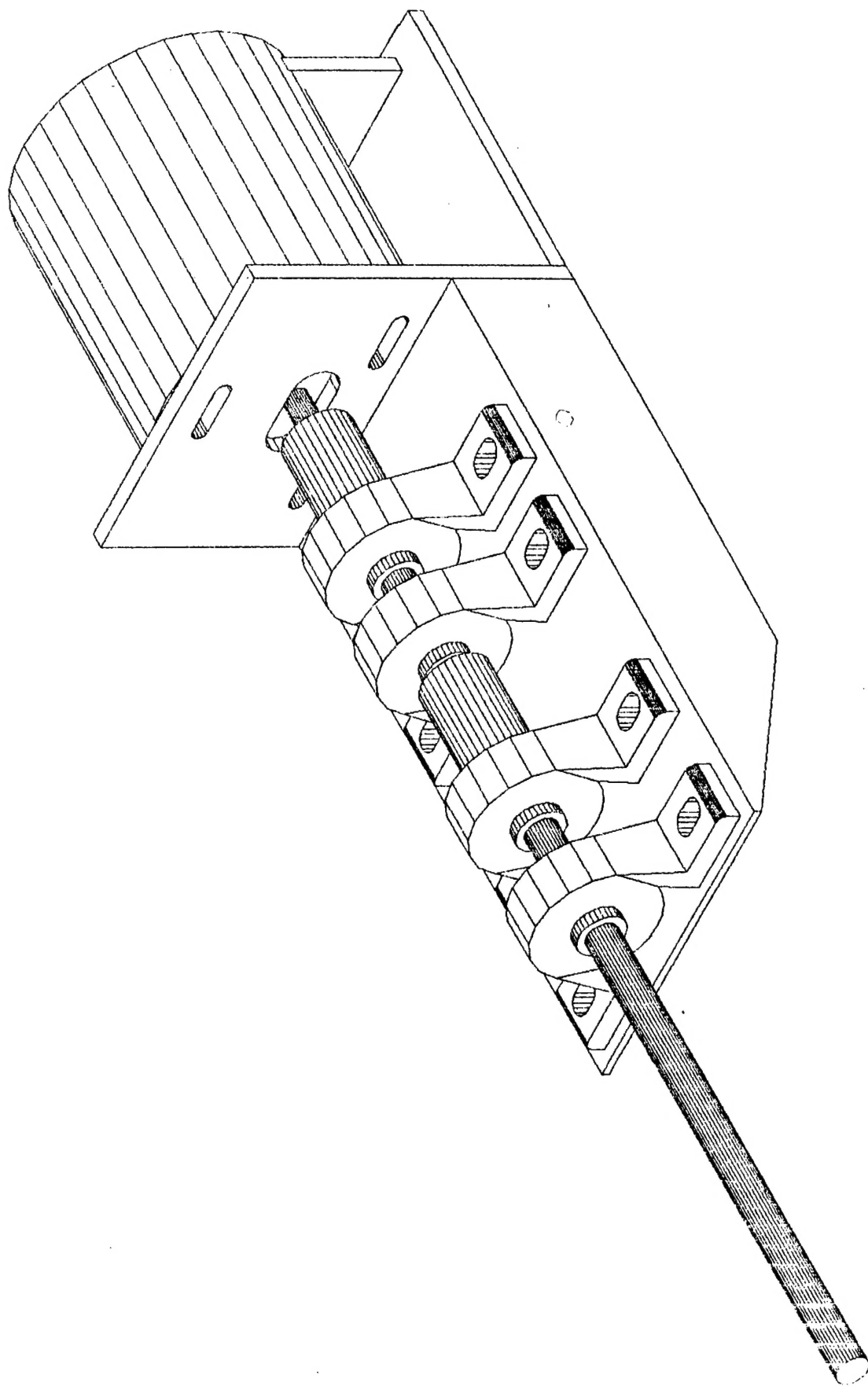


Fig. 1. The dynamic roll actuator/loadcell mechanism.

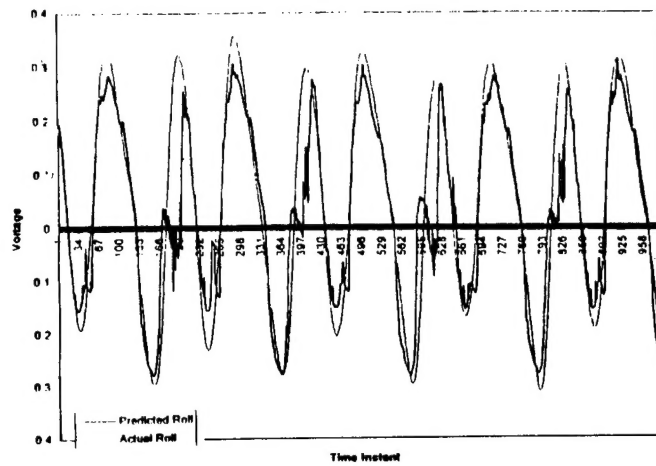


Fig. 2. Predicted and actual roll of the model at a wave incidence of 15° and a frequency of 0.5 Hz.

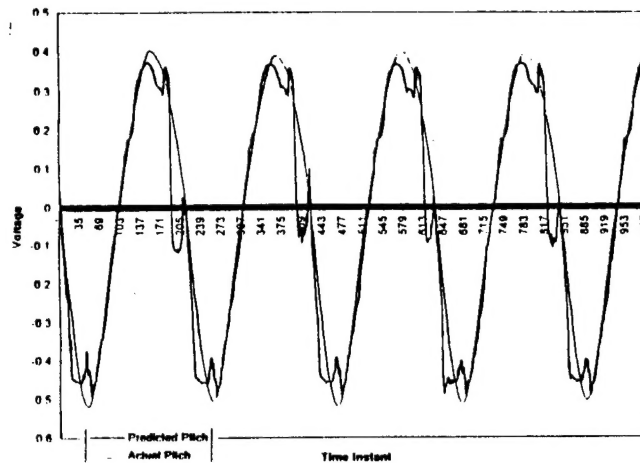


Fig. 3. Predicted and actual pitch of the model at an incidence of 15° and a frequency of 0.5 Hz.

APPENDICES

Appendices are attached only to the copy
submitted to the technical monitor

Appendix I:

This is a very long document, so was not included in this transmission; it is available at your request.

Appendix II

Fuzzy Logic & Neural Network System Identification for High Alpha Delta Wing Maneuvers with Deployable Control Surfaces

Deborah A. Furey** and O. K. Rediniotis†
Department of Aerospace Engineering
Texas A&M University
College Station, TX

and

Christopher T. Moore*, Norman W. Schaeffer*, and Demetri P. Telionis††
Virginia Polytechnic Institute and State University
Blacksburg, VA

Abstract

Fuzzy logic and neural network system-identification and control techniques are employed in high-alpha delta-wing unsteady aerodynamics. A delta wing, equipped with cavity flaps or an apex flap, is executing pitch-up maneuvers while the flaps are dynamically employed, aiming to modify and control the behavior of the two leading-edge vortical structures and thus their effect on the pressure distribution and aerodynamic loading of the wing. First a fuzzy identifier is constructed to predict the temporal evolution of the leeward pressure distribution and the aerodynamic loads for given time histories of pitching, $\alpha(t)$, $\dot{\alpha}(t)$ and flap deployment $\phi(t)$, $\dot{\phi}(t)$.

Introduction

The aerodynamics of supermaneuver-performing aircraft has been a great challenge to aerodynamicists but still many questions in this area are unanswered. This is partly due to shortage of wind-tunnel hardware able to simulate complex maneuvers of sensor-instrumented models and allow the measurement of the properties of the model flowfield interaction. Moreover, when the control of these interactions is desired, the task becomes understandably overwhelming: different flow-control devices have to be tested, each one at several different dynamic deployment schedules and rates, as well as testing of combinations of flow-control devices. While a sufficiently large data bank of these

test data has been generated, then the daunting question emerges: How is all this information efficiently implemented into the next generation super-agile aircraft? Since the rapid rates of motion during a supermaneuver are beyond the pilot's response limits, an active controller between the pilot and the aircraft is necessary. To reinforce the gravity of the problem, along comes the inadequacy of the conventional adaptive control schemes: the high rates and large motion amplitudes involved in a supermaneuver preclude the local linearization of the strongly nonlinear governing equations.

Schreck et al¹ demonstrated application in unsteady aerodynamics of system-identification and modern control methods based on the use of artificial neural networks (ANN). There^{1,2}, ANNs were shown to successfully model vortex dynamics principles. Further attempts were also reported later^{3,4}. Fuzzy logic systems (FLS) appear to be equally capable system identifiers. Comparisons of the two techniques^{4,5}, i.e., ANN versus FLS in different applications seem to favor the latter. However, we believe that neural networks and fuzzy logic have complementary strengths and a symbiotic relationship between the two holds the secret to effective system identification and control.

In this paper we first demonstrate that FLS and ANN can successfully identify non-linear aerodynamic systems. Our system consists of a pitching delta wing with dynamically deployed flaps during the maneuver. We identify the effect this system has on the temporal evolution of the leeward-side pressure distribution as well as the aerodynamic loads. Once a system model has been generated a fuzzy controller will be constructed with the objective to control the cavity-flap deployment schedule during pitch-up, so that a certain optimisation criterion is satisfied, for example, the maximising of the ratio L/D (lift over drag) for all times during the maneuver.

** Research Associate

† Asst. Professor, Member AIAA

* Research Assistant

†† Professor, Associate Fellow AIAA

Copyright © 1996 by the American
Institute of Aeronautics and
Astronautics, Inc. All rights reserved.

Facilities and Instrumentation

The present research was conducted in the VPI & SU Stability Wind Tunnel and the ESM Wind Tunnel. The first has a 6' x 6' test section and an excellent quality of flow. This tunnel has been recently equipped with a dynamic strut which was given the acronym DyPPiR for "Dynamic-Plunge-Pitch-Roll" mechanism. The design, construction and calibration of this facility involved many faculty at VPI&SU, under the direction of Dr. Roger Simpson and five years of intensive work. A discussion of the main elements of the design can be found in Ref. 6 and the accompanying instrumentation in Ref. 7.

The DyPPiR can provide simultaneous plunging, pitching and rolling of models on the order of 100 lb in weight, at a frequency of up to 10 Hz, depending on the amplitude of the motion. These motions can be independently controlled by software. Any combination of arbitrary motions is possible. In this case, pitch up motions are executed. Such motions have been tested earlier in two much smaller facilities^{8,9}, a wind tunnel and a water tunnel and at Reynold numbers of the order of 10^4 . Simultaneous plunging of the DyPPiR carriage and pitching of the pitch actuator induces pitching of the model about its quarter-chord axis. The aim here is to control the leading edge vortices and delay breakdown, while pitching up to high angles of attack. This is pursued by deploying cavity flaps.

In the present experiments we employ a 2' x 3' delta wing model (Fig. 1) which has been tested extensively in this facility in steady flow⁷. The model is hollow to provide space for instrumentation. The top surface of the model is equipped with three rows of pressure taps. Pressure transducers are positioned beneath the instrumented surface to provide unsteady pressures with a high frequency response. Fifteen pressure ports were aligned with a normal to the leading edge, at a distance of $x/c = 0.61$ from the apex. A 32-transducer Electronic Pressure Scanner (ESP) from PSI, Inc. with a pressure full scale of ± 20 in H_2O was employed. The ESM Pressure Scanner was interfaced with a laboratory computer and was on-line calibrated through instrumentation by AEROPROBE Corp. The system consists of an ESP interface/data-acquisition board PDA-3101 (31 KHz max sampling rate) and an ACCUPRES computer-controlled, on-line pressure calibrator. Figures 2(a) and 2(b) present the coordinate system used and the pressure port distribution, respectively.

Fuzzy Logic Systems (FLS)

A recently developed field in mathematics, the theory of fuzzy sets and the logic stemming from it has been gaining ground as a system identifier, sometimes at the expense of ANN popularity. In fact, in the semiconductor industry, microcontroller pundits predict that semiconductor-based fuzzy technology will be as prevalent in products by the end of the decade as microprocessor technology is today. Although traditionally, fuzzy logic has been viewed as a technique for representing imprecise, ambiguous and vague information, nothing prevents it from successfully dealing with concrete, quantitative and precise data. In fact, the Universal Approximation Theorem stated below proves that fuzzy logic systems are capable of uniformly approximating any nonlinear function to any degree of accuracy.

Figure 3 presents a schematic of the basic configuration of the fuzzy logic systems proposed in this work. The fuzzy rule base consists of a collection of fuzzy if-then rules in the following form:

$R^{(\ell)} : \text{If } x_1 \text{ is } F_1^{\ell} \text{ and } \dots \text{and } x_n \text{ is } F_n^{\ell}, \text{ THEN } y \text{ is } G^{\ell},$

where F_i^{ℓ} and G^{ℓ} are fuzzy sets,

$\mathbf{x} = (x_1, \dots, x_n)^T$, y are the input and output linguistic variables, respectively, and $\ell = 1, \dots, M$ with M being the numbers of rules.

However, in engineering systems, inputs and outputs are real-valued variables in crisp sets and not linguistic variables in fuzzy sets. The conversion from the former to the latter and vice-versa is achieved through the fuzzifier and defuzzifier respectively. The fuzzy inference engine is the heart of the system and maps the fuzzy inputs to the fuzzy outputs, properly employing the rules from the fuzzy rule base. In one of our approaches we use center average defuzzifier, product-inference rule, singleton fuzzifier and Gaussian membership function. Then the fuzzy system reduces to:

$$f(\underline{x}) = \frac{\sum_{\ell=1}^M y^{\ell} \left[\prod_{i=1}^n a_i^{\ell} \exp \left(- \left(\frac{x_i - \bar{x}_i^{\ell}}{\sigma_i^{\ell}} \right)^2 \right) \right]}{\sum_{\ell=1}^M \left[\prod_{i=1}^n a_i^{\ell} \exp \left(- \left(\frac{x_i - \bar{x}_i^{\ell}}{\sigma_i^{\ell}} \right)^2 \right) \right]} \quad (1)$$

where $\underline{x} = (x_1, \dots, x_n)^T \in U$ (U is the universe of discourse) is the input vector, n is the number of antecedents (inputs) and M is the number of rules. $\bar{x}_i^{\ell}, \sigma_i^{\ell}, a_i^{\ell}$ are the parameters of the Gaussian membership functions and y^{ℓ} are the centers of the output fuzzy sets. Although our techniques are capable

of identifying multi-input, multi-output systems, here to facilitate the reader's understanding, a multi-input, single-output system is presented. We state here the following University Approximation Theorem⁴:

For any given real and continuous function g on a compact set $u \in R^n$ and arbitrary $\epsilon > 0$ there exists a fuzzy logic system f in the form of (A) such that

$$\sup_{x \in U} |f(x) - g(x)| \leq \epsilon.$$

Generating rules and membership functions for fuzzy logic is essentially a learning process. Here is where the utilization of neural network techniques enters our modeling process. Using supervised learning, a neural network can generate or sort out rules and tune the membership function parameters. For instance, for the single-output system (A) training is achieved using a back-propagation algorithm to determine the parameters \underline{x}_i^t , σ_i^t , y^t (without loss of generality the α_i^t 's are set equal to 1).

Fuzzy Logic Training Algorithm

Wang [4] shows that the fuzzy logic system given by Eqn. (1) is an optimal fuzzy logic system in the sense that the Gaussian shape variable, σ , can be chosen such that the output of the fuzzy logic system matches any given N input-output pairs to any given accuracy. A nearest neighborhood clustering algorithm is used to train the system starting with the first input-output pair. A cluster center is established and a cluster radius is chosen. If the distance between any subsequent input-output pair and the current cluster is greater than the cluster radius, then a new cluster center, or fuzzy rule, is established. This continues until all training I-O pairs are used. The fuzzy logic system thus has two independent variables, the cluster radius and the Gaussian shape variable, which must be chosen before the system can be trained. These variables greatly affect the complexity and accuracy of the fuzzy logic system and will vary based upon the needs of the user.

The cluster radius determines the minimum amount that one point in the training data must differ from all other points in order to be part of a new fuzzy rule. The advantage of this clustering method is that for any given system and cluster radius there is a limit to the number of fuzzy rules which can be created. Thus the cluster radius directly determines the

complexity of the fuzzy rule base for any given system. In this study, the amount of training data was minimal. For this reason, the cluster radius was usually chosen small enough such that every input-output pair created a new fuzzy rule.

The Gaussian membership function shape variable is a smoothing variable. If the Gaussian shape variable is large, then it has a smoothing effect and the result will be a very generalized fuzzy logic system. This may be useful in systems where data are noisy but could have an adverse effect on complex systems. If the Gaussian shape variable is small, then predicted outputs will have nearly the same magnitude as the closest training cluster center, particularly when the training data is sparse. Thus a compromise between generalization and accuracy must be made, depending on the complexity of the system, quality of data, and sparseness of data. It is generally not difficult, however, to determine an appropriate value for the Gaussian shape variable through a few trial-and-error procedures.

Neural Network Training Algorithm

Using the pitch-up delta wing data, a neural network was trained to predict the spatial and temporal pressure coefficients on the surface of the wing. Data were provided for four pitch-up rates, 22°/s, 40°/s, 48°/s, and 66°/s, in the form of pressure coefficients for 15 pressure ports. The ports were equally spaced from the centerline of the delta wing out to the leading edge. Pressure profiles for several instantaneous angles of attack in each pitch-up schedule provide the input data for the neural network.

The network was trained using backpropagation. A three-layer (two hidden layers) network was used for the present study (Fig. 4).

The input vectors consist of port number, instantaneous wing angle, $\alpha(t)$, and pitch rate, $\dot{\alpha}(t)$. The fact that the pressure ports are equally spaced allowed for use of the port number (integer from 1 to 16) as a network input instead of each port's actual distance from the leading edge. The network output is the instantaneous pressure coefficient $C_p(t)$. The first and second hidden layers consisted of 8 and 4 neurons, respectively, with log-sigmoid activation functions. The output layer consisted of one neuron with linear activation function. The functional description of the log-sigmoid activation function is:

$$G(x) = \frac{1}{1 + e^{-x}} \quad (2)$$

The linear activation function is:

$$G(x) = Ax + b \quad (3)$$

where x is the input value. The backpropagation method utilized Levenberg-Marquardt optimization techniques. This approach uses an approximation of Newton's method for updating the weighting coefficients. The Levenberg-Marquardt weight update rule is:

$$\Delta W = (J^T J + \omega I)^{-1} J^T \epsilon \quad (4)$$

where J is the Jacobian matrix of the derivatives of error with respect to weight and ϵ is the error vector. The scalar multiplier, ω , influences the update rule. When ω is large, the update rule is approximately the gradient descent method and when ω is small, the update rule approximates the Gauss-Newton method. The multiplier is adjusted in the back propagation training procedure to maintain small errors. This technique allows for faster convergence than a purely gradient descent method.

Results

The results in this study were produced from two sets of training data. The first set was obtained on the DyPPiR apparatus in Virginia Tech's stability tunnel and contains pressure coefficients at spanwise pressure ports across half of a pitching delta wing for various pitch-up rates. The ports are located at $x/c = 0.61$. Thus, when training with these data, the fuzzy logic system was given port number p_i , pitch-up rate α , and angle of attack α , as inputs with the pressure coefficient as the desired output. The second set of data were obtained in Virginia Tech's ESM wind tunnel and contains pressure coefficients across the entire span of a pitching delta wing for various cavity flap deployment schedules. The cavity flap deployment schedules consisted of pitch-up motions from 28° to 61° with flaps not deployed, deployed at 32° , deployed at 40° , and always deployed. When training the fuzzy logic system with these data, the system was given port number, time, angle of attack, and a deployment flag (0 if not deployed, 10 if deployed) as inputs with the pressure coefficient as the desired output.

First the fuzzy logic system was trained using the DyPPiR data with all pitch-up rates and angles of attack except for the angles of attack of 36.02° and 44.04° for the pitch-up rate of 48.6 degrees per second. The trained system was then used to predict the pressure distributions at the missing angles and the

results are shown in Figs. 5 and 6. Note that several different values were used for the Gaussian shape variable in order to show how the system responds to variations of this parameter. Figure 7 shows the actual pressure distributions over the wing at 36.02° as well as at the prior and following angles of attack and also the interpolated curve between these two. It is necessary to examine these curves to avoid the impression that the fuzzy logic system is simply an averaging system.

In an attempt to increase the accuracy of the fuzzy logic predictions at the angle of attack of 44.04° , the system was retrained with the pressure coefficient at port 3 for the target angle included in the training data. The results from this training are shown in Fig. 8. The system was then retrained adding one more point at the target angle until four additional points were included beyond those used in the initial training. These results, shown in Fig. 9, would indicate that a well trained system would be able to accurately predict the pressure distribution over an entire wing with only a small sample of the pressures over the wing.

In order to allow for comparisons between the fuzzy logic and neural network identification systems, the system was then trained with all of the data obtained from the DyPPiR apparatus. The trained system was then used to predict all of the spanwise pressure distributions for each angle of attack included in the 48.6°/s pitch-up rate data files. Since all of the predicted values were included in the training data, it is expected that the fuzzy logic predictions should exactly match the actual data. It can be seen in Fig. 10 that the predicted values do indeed correspond exactly with the actual data values. These results may not be significant from a potential controls standpoint but they do verify that the fuzzy logic training algorithm is functioning as expected.

Next the system was retrained using every other point from the data files for all five pitch-up schedules. The fuzzy logic model was then once again used to predict pressure distributions, shown in Figure 11, for all angles of attack for the 48.6°/s pitch-up rate. In order to form an accurate model, it was necessary to use a value of 1.5 for the Gaussian shape variable in the training of the fuzzy logic system. The necessity of such a large value for this variable indicates that the training data set is becoming sparse and does not bode well for the success of a more widely distributed set of data.

The system was then trained one final time using every third point from the data files for every pitch-up

schedule. Once again the fuzzy logic model was used to predict the pressure distributions for the $48.6^\circ/\text{s}$ pitch-up rate. In order to even closely approximate the original data, it was necessary to use a value of 2.0 for the Gaussian shape variable. Although the predicted data does follow the original data fairly well, as seen in Fig. 12, the model does demonstrate ripple and undershoot. This is a characteristic of a model which is too generalized as a result of using a large Gaussian shape variable to counteract a sparse training data set.

In an effort to test the effectiveness of the fuzzy logic system when used in conjunction with control surfaces, the system was trained with three of the four available cavity flap deployment schedules. The system received as input the data from the always deployed and never deployed schedules in addition to the 32° deployment schedule. The resulting fuzzy logic model was then used to predict pressure distributions at all times for the 40° deployment schedule. Figure 13 shows a spectral plot of the absolute error between the actual and predicted values for all spatial and temporal locations. It can be seen that the error is relatively small for all times with a maximum error occurring at approximately 0.4 seconds. Figure 14 shows the actual and predicted pressure distributions for this maximum error case. Figure 15 through 18 show the actual and predicted pressure distributions at quarter second intervals and Fig. 19 shows the pressure distribution immediately following the deployment of the cavity flaps. All of these predictions are good approximations of the actual data considering the limited amount of available training data.

Finally, it was desired to test the fuzzy logic system with an extremely limited amount of training data. To achieve this purpose the system was first trained with the full data sets from the fully deployed and never deployed cavity flap schedules in addition to all the data from ports 3 and 7 from the 32° and 40° deployment schedules. The resulting model was then used to predict the pressure distributions for the 32° and 40° deployment schedules for all spatial and temporal locations. The error spectrum resulting from these two sets of predicted data are presented in Figs. 20 and 21. The process was then repeated with the addition of data from port 2 from the 32° and 40° deployment schedules and then again including port 6. The error spectrum plots for the three point training are shown in Figs. 22 and 23 and those from the four point training in Fig. 24 and 25. Although the magnitude of the maximum error does not decrease as the number of training points increases, it is observed

from the error spectra that the overall error of the model does decrease as the complexity of the training is increased. The maximum error and quarter second pressure distributions for the four point predictions of both the 30° and 40° deployment schedules can be seen in Figs. 26 through 35. Although these results stray somewhat from the original data, they are still encouraging in light of the limited number of deployment schedules available for training the system.

The neural network was first trained also with the entire available database. The intention here was to show whether or not an accurate model for the aerodynamic system could be found in the first place, that could match the existing data. This process led us in heuristically identifying a network architecture (layer and neuron arrangements, activation functions, etc.) that performed optimally. The trained network was then used to predict the pressures at intermediate ports (port numbers 2.5, 3.5, etc.) to ensure that the model was not ill-behaved between the training data, although experimental data was not available at such ports. The results are presented in Fig. 36. For all angles of attack and port locations, there is excellent agreement between the predicted pressure coefficient from the trained network and the actual data. The above graphs show that the predicted values for these conditions are consistently within an acceptable accuracy.

Figure 37 presents predictions with training performed on the network using every other point from the data files for each pitchup schedule. The above graphs show the results for the pitchup rate of $48^\circ/\text{sec}$. There is good agreement for all angles of attack and port locations between the predicted output pressures and the actual data with some regions where the model accuracy is compromised. For this training condition, the network is trained with fewer data points but overall, still predicts output values within acceptable accuracy over the entire spatial (port number) and temporal (angle of attack) ranges.

Results of training performed on the network using every third point from the data files for each pitchup schedule are presented in Fig. 38. The graphs show the results for the pitchup rate of $48^\circ/\text{sec}$. It should be noted that the overall model prediction capability is still very good.

Figure 39 shows the results from training the network with 50 randomly selected points from the data for the pitchup rate of $48^\circ/\text{sec}$. Agreement is very good for most angles of attack and pressure ports.

Finally, training was carried out using half of all the data for all the pitch-up rates. Figure 40 shows predicted vs. actual data for pitch rate of 22 deg/sec and Fig. 41 for pitch rate of 40 deg/sec.

Conclusions

A fuzzy logic and neural network system were trained with pressure data obtained experimentally over a maneuvering delta wing. This was essentially a feasibility study to demonstrate the sensitivity of each technique to the number of available data for training.

It is indicated that highly non-linear phenomena can be quite accurately predicted. The power of such methods is that once a system is trained, then a minimum number of input sensors is necessary to generate a new prediction. The practical importance of such a scheme is that a system can be trained by flight data. Four or five sensors on a prototype aircraft will be enough to generate accurate prediction which could be used to activate computerized control of the aircraft attitude. This idea was tested by provided information at only four pressure portions and requiring the system to predict the overall pressure distribution.

A great advantage of such systems is that training can be carried out on board and, in fact, continuously improved as more data becomes available. This is presently being simulated.

Acknowledgements

This work was supported by the Air Force Office of Scientific Research, Project No. AFOSR-91-8310 and ASSERT Project No. F49620-93-1-0455 and was monitored by Major Daniel Fant and later by Dr. James McMichael.

References

1. Schreck, S. J., Faller, W. E., and Luttges, M. W., "Neural Network Prediction of Three-Dimensional Unsteady Separated Flow Fields," AIAA Paper No. 93-3426-CP, Monterey, CA, August 1993.
2. Faller, W. E., Schreck, S. I., Luttges, M. W., "Real-Time Prediction and Control of Three-Dimensional Unsteady Separated Flow Fields Using Neural Networks," AIAA Paper No. 94-0532, Reno, Nevada, Jan. 1994.
3. Steck, J. E., and Roehsat, K., "Use of Neural Networks in Control of High Alpha Maneuvers," AIAA Paper No. 92-0048, Reno, NV, Jan. 1992.
4. Wang, Li-Xin, "Adaptive Fuzzy Systems and Control, Design and Stability Analysis," Prentice Hall, New Jersey, 1994.
5. Kosko, Bart, "Neural Networks and Fuzzy Systems," Prentice Hall, New Jersey, 1992.
6. Ahn, S., Choi, K.-Y., and Simpson, R. L., "The Design and Development of a Dynamic Plunge-Pitch-Roll Model Mount," AIAA Paper No. 89-0048, 1989.
7. Rediniotis, O. K., Hoang, N. T., and Telionis, D. P., "Multisensor Investigations of Delta Wing High-Alpha Aerodynamics," AIAA Paper No. 91-0735, 1991.
8. Rediniotis, O. K., Klute, S. M., Hoang, N. T., and Telionis, D. P., 1992, "Pitch Up Motions of Delta Wings," AIAA Paper No. 92-0278, 1992, also *AIAA Journal*, in press.
9. Hoang, N. T., Rediniotis, O. K., and Telionis, D. P., "Three-D LDV Measurements Over a Delta Wing in Pitch-Up Motion," AIAA Paper No. 93-0185, 1993.

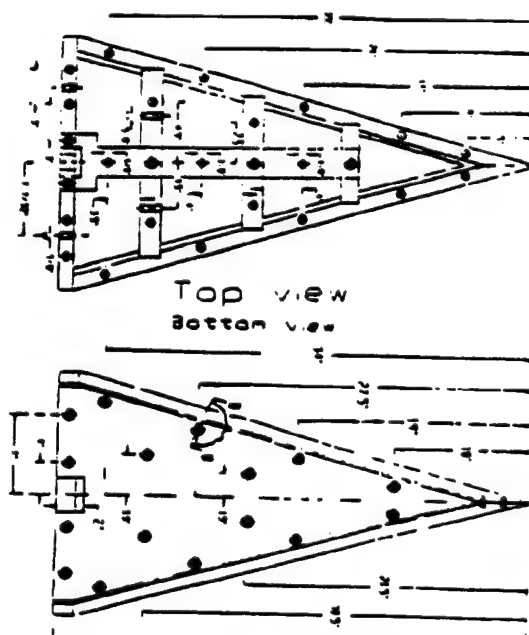


Fig. 1: The delta wing model.

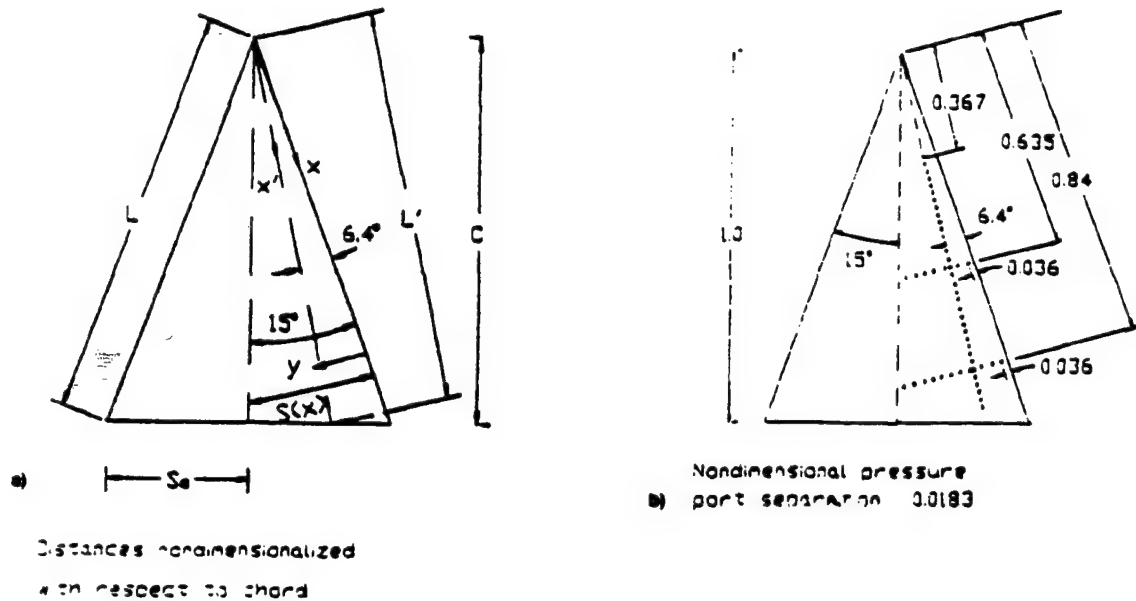


Fig. 2: Coordinate systems used for the pressure data and pressure port distribution on the leeward side of the model; all dimensions are reduced by the chord length C .

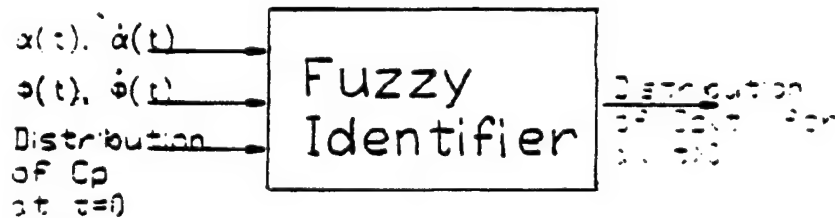


Fig. 3: The fuzzy system identifier.

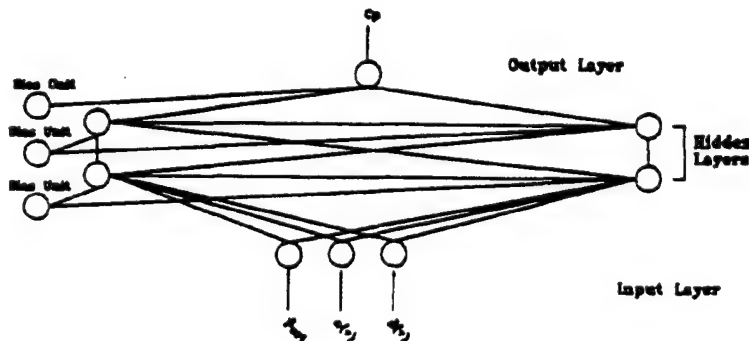


Fig. 4: Schematic of three layer neural network.

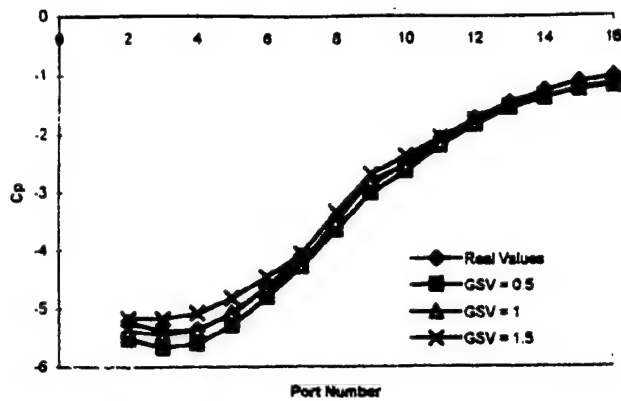


Fig. 5: Pressure Distribution across pitching delta wing. Real and trained results shown for varying Gaussian shape variables @ $\alpha = 36^\circ$

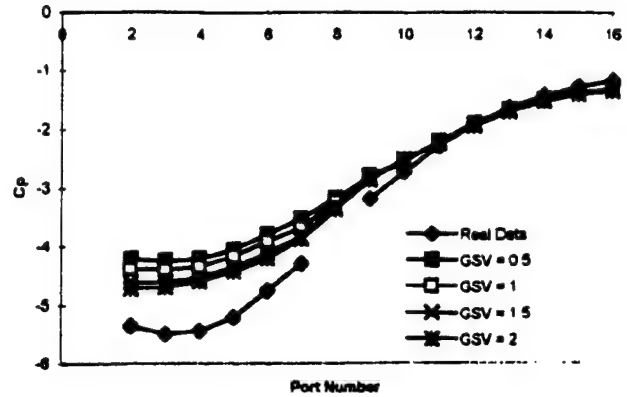


Fig. 6: Pressure Distribution across pitching delta wing. Real and trained results shown for varying Gaussian shape variables @ $\alpha = 44^\circ$

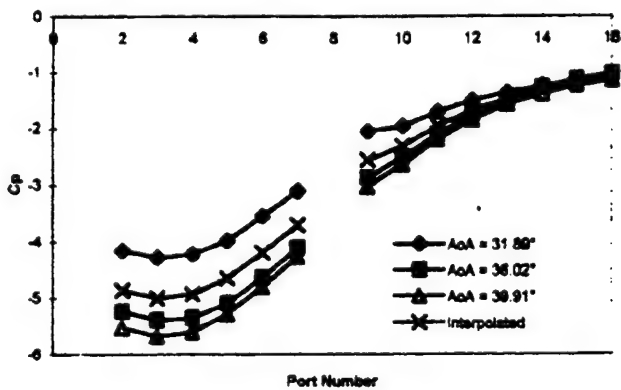


Fig. 7: Pressure Distribution across pitching delta wing for $\alpha = 32^\circ$, 36° , and 40° plus curve interpolated from 32° and 40° curves.

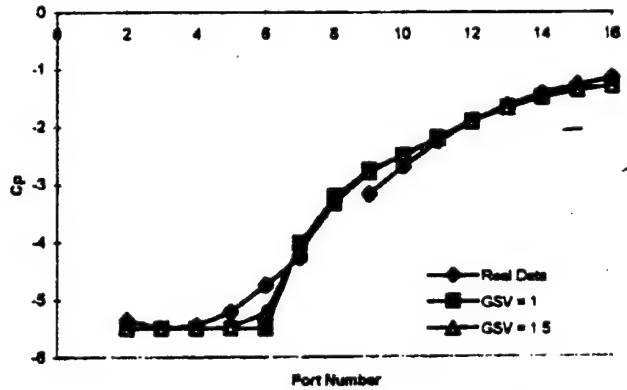


Fig. 8: Pressure Distribution across pitching delta wing. Real and trained results shown for varying Gaussian shape variables w/ one training point in target space @ $\alpha = 44^\circ$

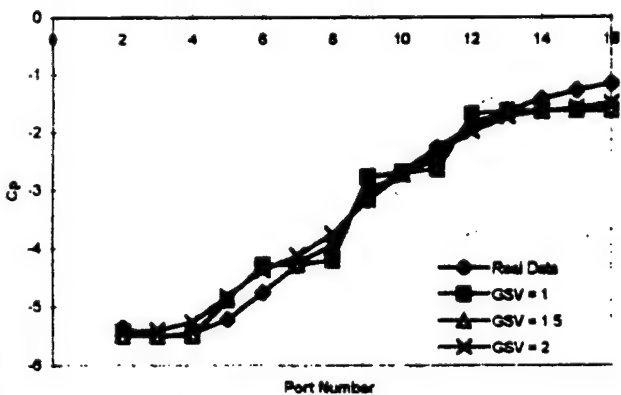


Fig. 9: Pressure Distribution across pitching delta wing. Real and trained results shown for varying Gaussian shape variables w/ two training points in target space @ $\alpha = 44^\circ$

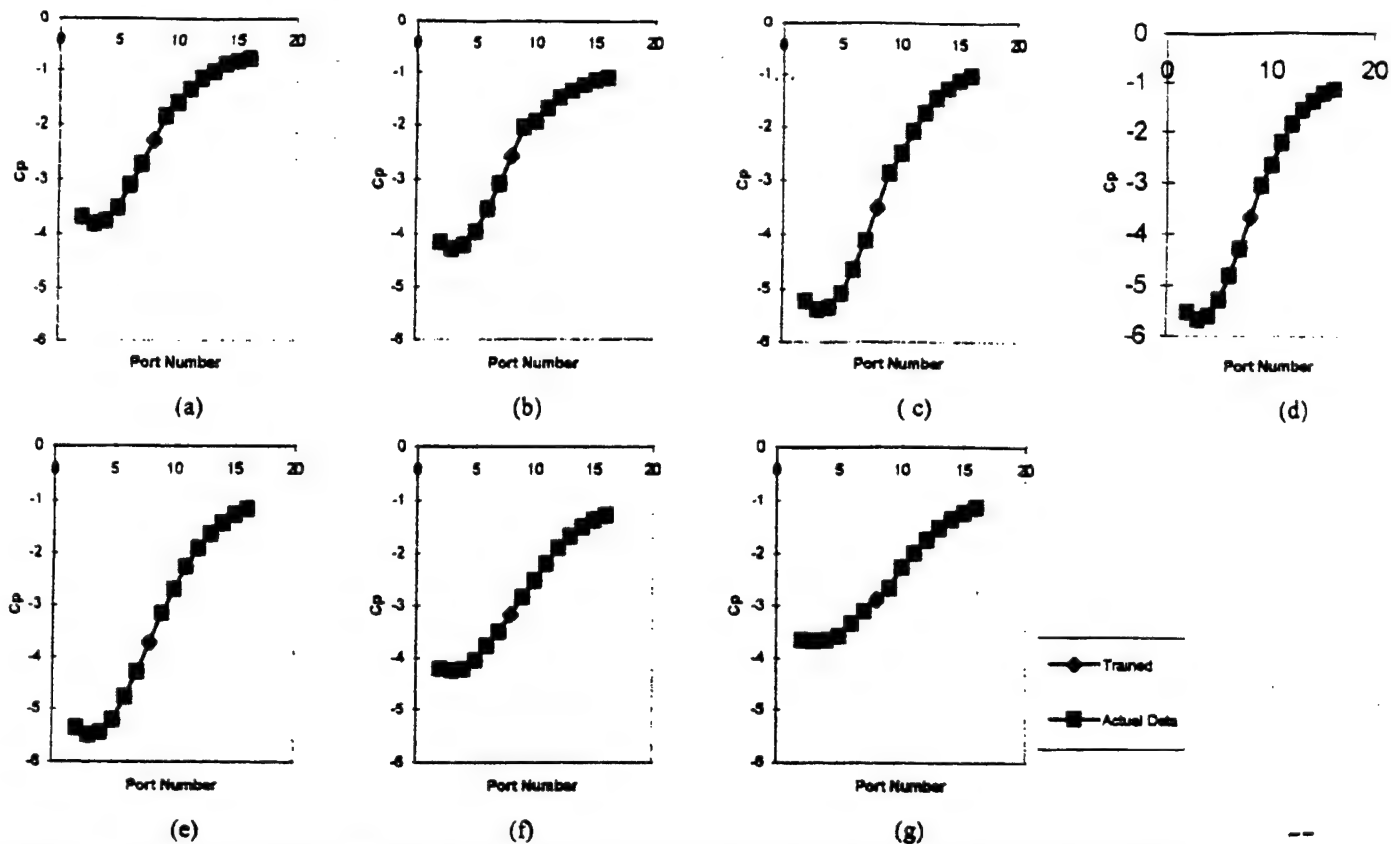


Fig. 10: Predicted and actual pressure distributions from fuzzy logic model trained at every point for pitchup rate of 48.6°/s at (a) $\alpha = 28^\circ$, (b) $\alpha = 32^\circ$, (c) $\alpha = 36^\circ$, (d) $\alpha = 40^\circ$, (e) $\alpha = 44^\circ$, (f) $\alpha = 48^\circ$, and (g) $\alpha = 50^\circ$.

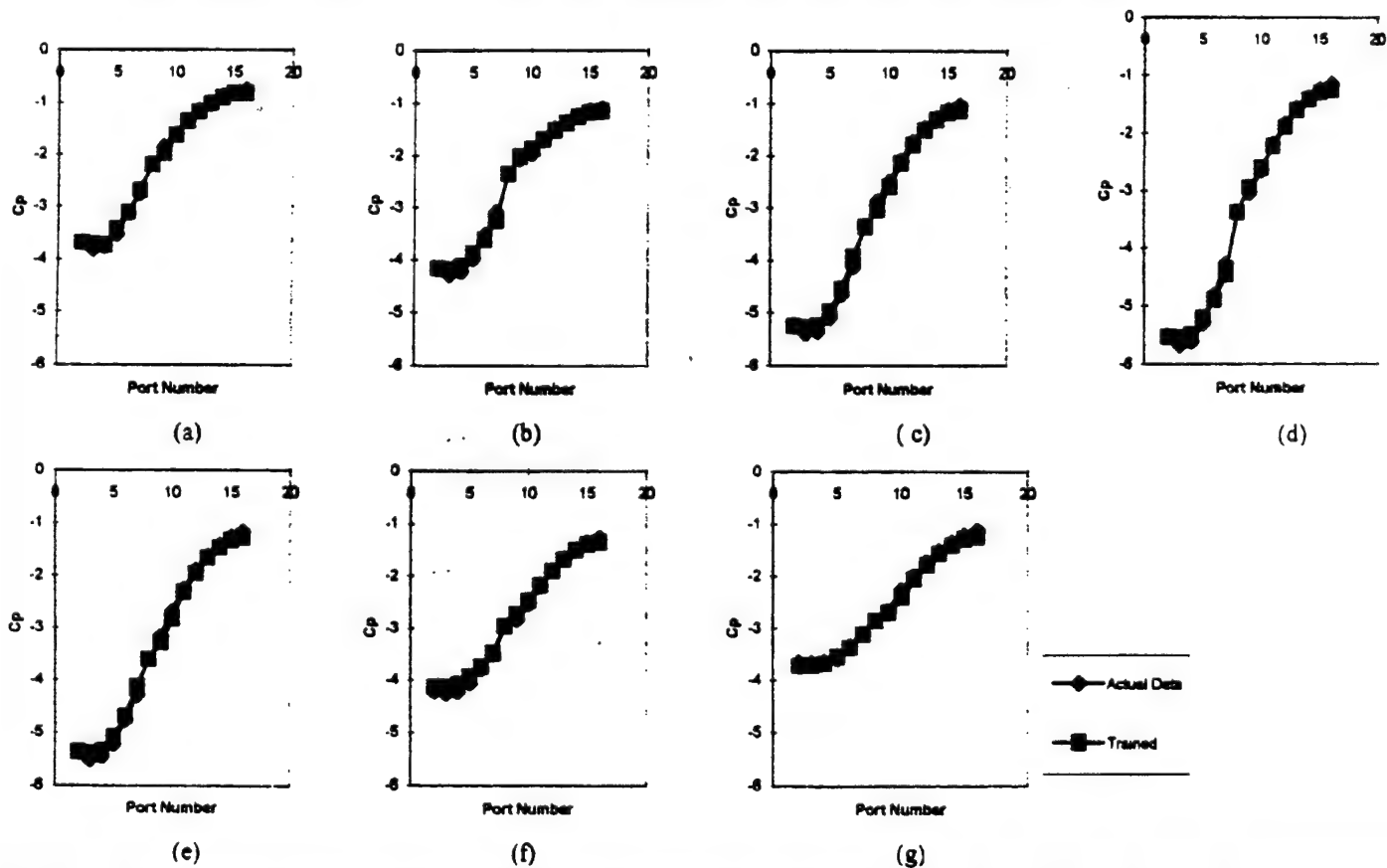


Fig. 11: Predicted and actual pressure distributions from fuzzy logic model trained at every other point for pitchup rate of 48.6°/s at (a) $\alpha = 28^\circ$, (b) $\alpha = 32^\circ$, (c) $\alpha = 36^\circ$, (d) $\alpha = 40^\circ$, (e) $\alpha = 44^\circ$, (f) $\alpha = 48^\circ$, and (g) $\alpha = 50^\circ$.

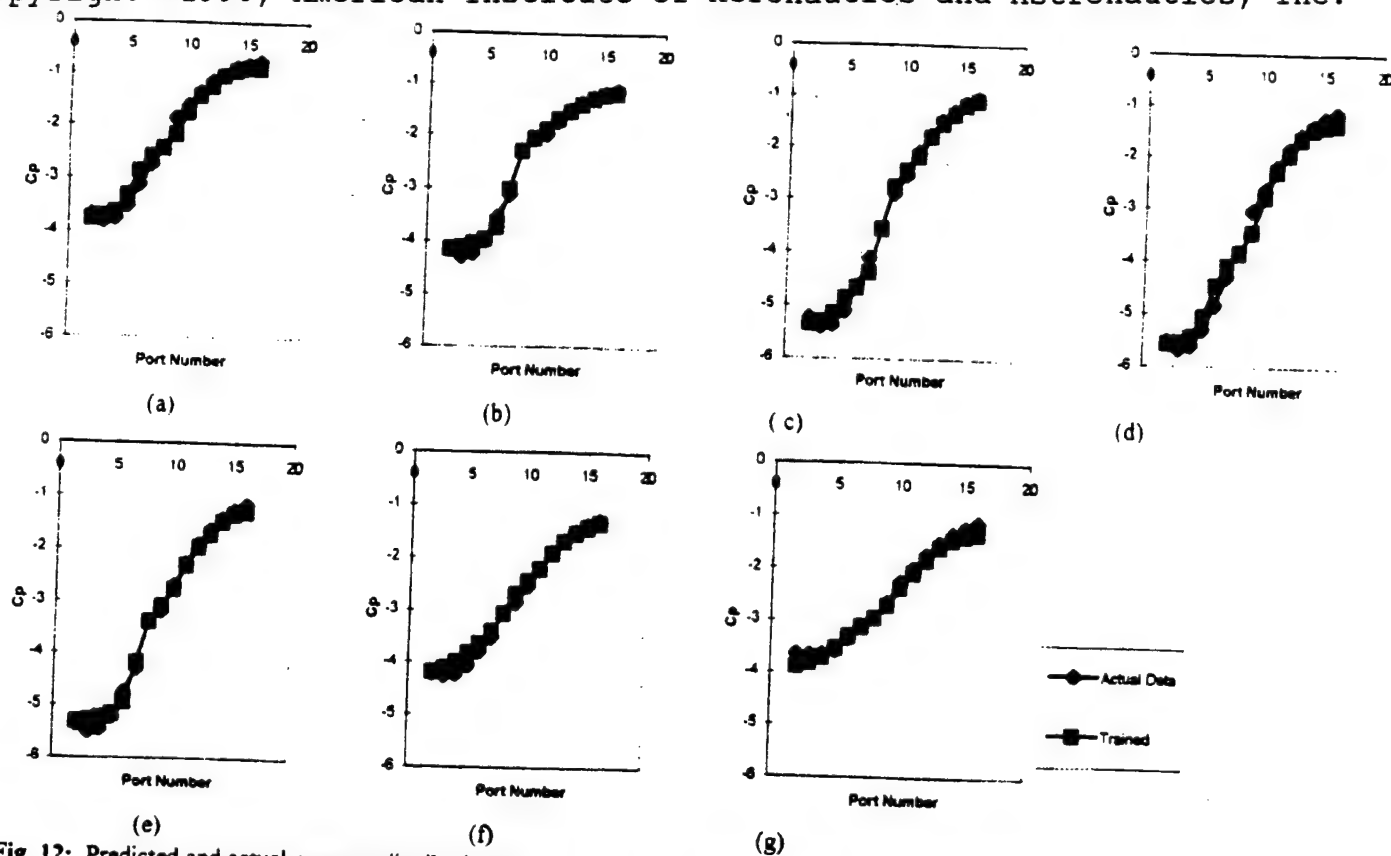


Fig. 12: Predicted and actual pressure distributions from fuzzy logic model trained at every other point for pitchup rate of $48.6^\circ/\text{s}$ at (a) $\alpha = 28^\circ$, (b) $\alpha = 32^\circ$, (c) $\alpha = 36^\circ$, (d) $\alpha = 40^\circ$, (e) $\alpha = 44^\circ$, (f) $\alpha = 48^\circ$, and (g) $\alpha = 50^\circ$.

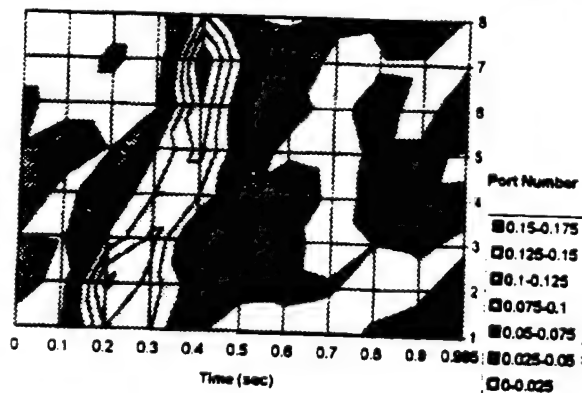


Fig. 13: Time record of fuzzy logic model error for 40° deployment schedule when trained with all other deployments.

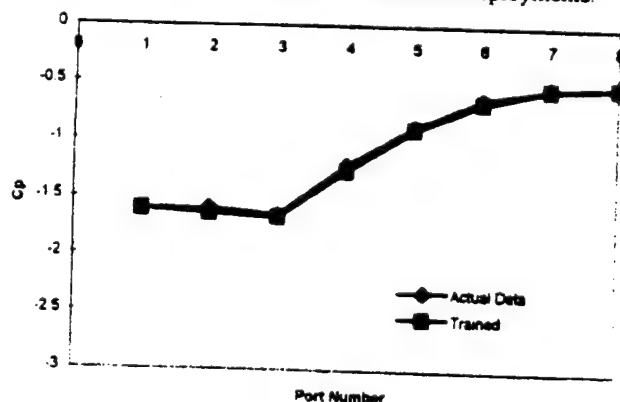


Fig. 15: Pressure distribution for Fig. 12 at time $t = 0\text{s}$.

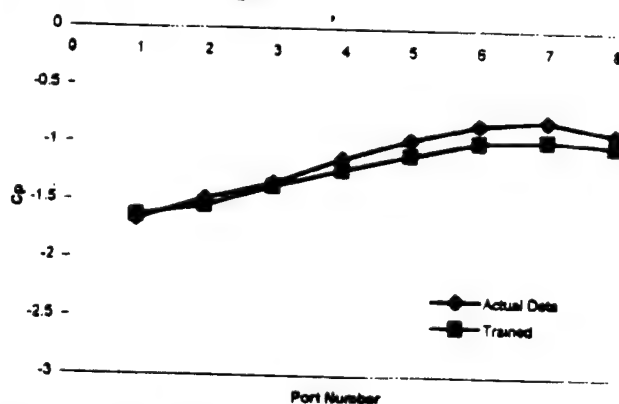


Fig. 14: Pressure distribution for Fig. 12 at time $t = 0.4\text{s}$ (Maximum error case)

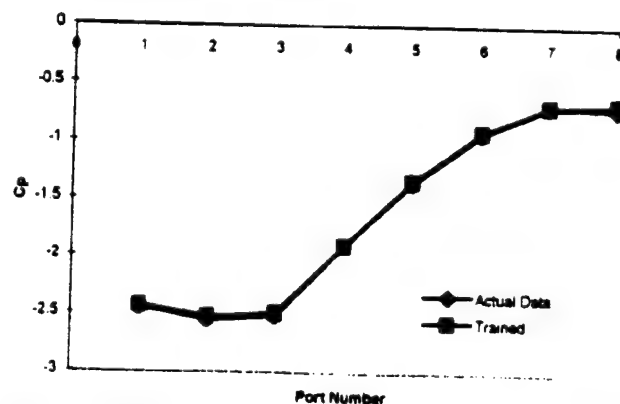


Fig. 16: Pressure distribution for Fig. 12 at time $t = 0.25\text{s}$

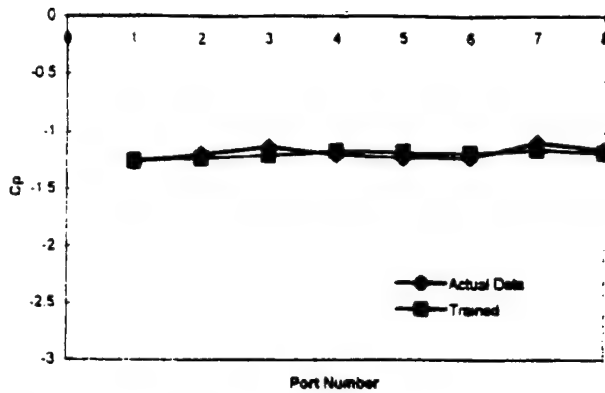


Fig. 17: Pressure distribution for Fig. 12 at time $t = 0.5s$.

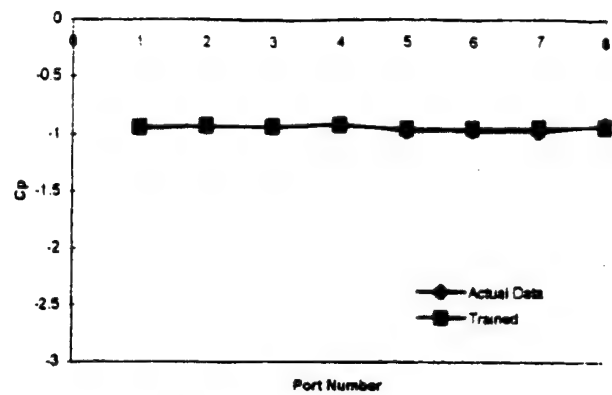


Fig. 18: Pressure distribution for Fig. 12 at time $t = 0.75s$.

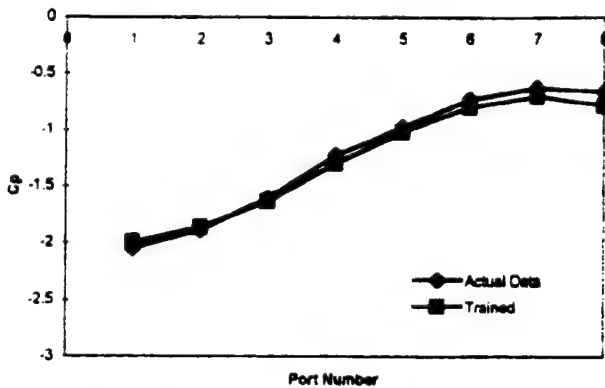


Fig. 19: Pressure distribution for Fig. 12 immediately following flap deployment. $t = 0.365s$.

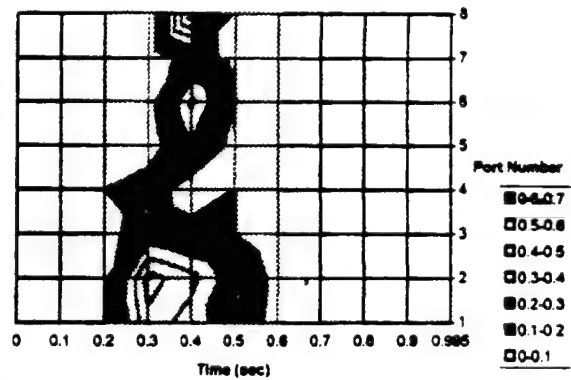


Fig. 20: Time record of fuzzy logic model error for 32° deployment schedule when trained with always and never deployed schedules in addition to ports 3 and 7 from 32° and 40° deployment schedules.

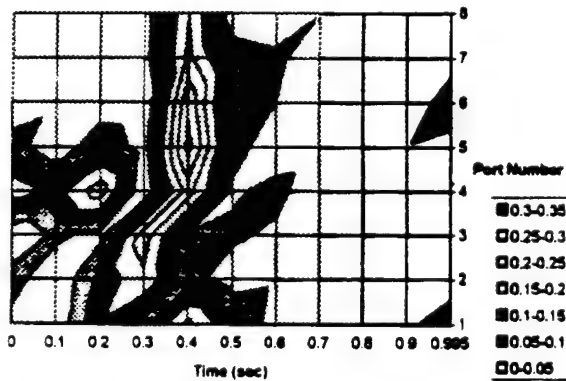


Fig. 21: Time record of fuzzy logic model error for 40° deployment schedule when trained with always and never deployed schedules in addition to ports 3 and 7 from 32° and 40° deployment schedules.

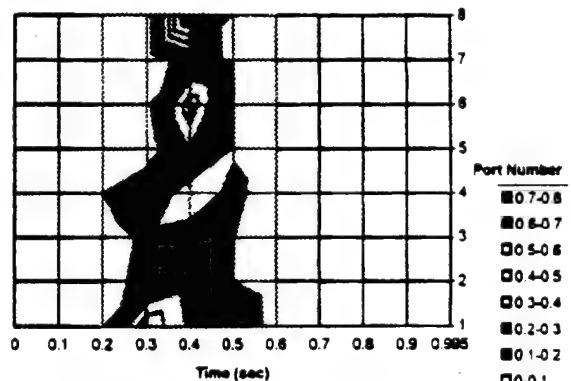


Fig. 22: Time record of fuzzy logic model error for 32° deployment schedule when trained with always and never deployed schedules in addition to ports 2, 3, and 7 from 32° and 40° deployment schedules.

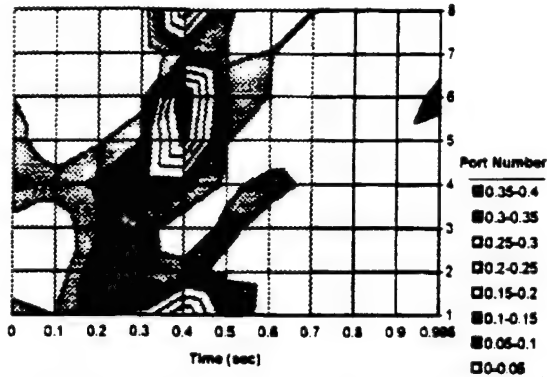


Fig. 23: Time record of fuzzy logic model error for 40° deployment schedule when trained with always and never deployed schedules in addition to ports 2,3, and 7 from 32° and 40° deployment schedules.

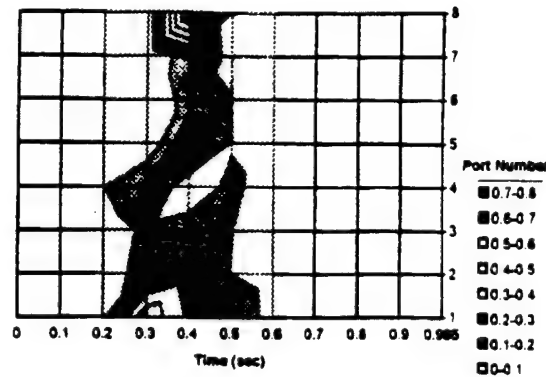


Fig. 24: Time record of fuzzy logic model error for 32° deployment schedule when trained with always and never deployed schedules in addition to ports 2,3,6, and 7 from 32° and 40° deployment schedules.

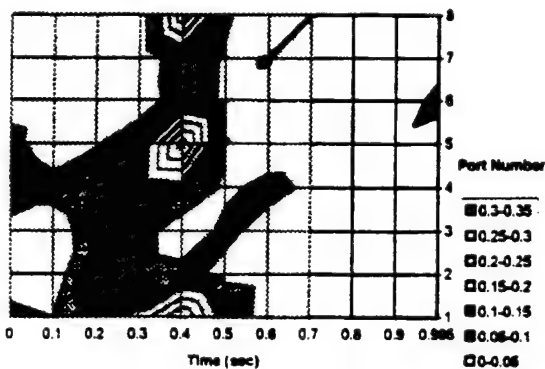


Fig. 25: Time record of fuzzy logic model error for 40° deployment schedule when trained with always and never deployed schedules in addition to ports 2,3,6, and 7 from 32° and 40° deployment schedules.

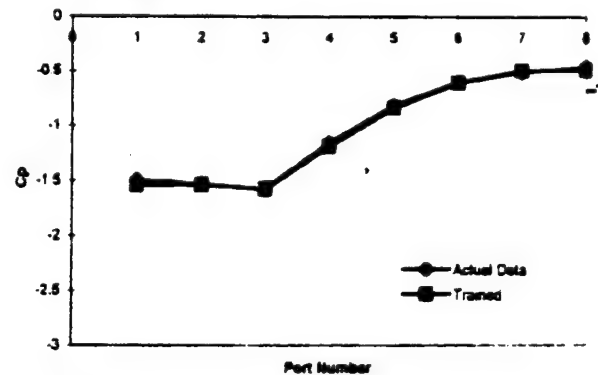


Fig. 26: Pressure distribution for Fig. 24 at time $t = 0s$.

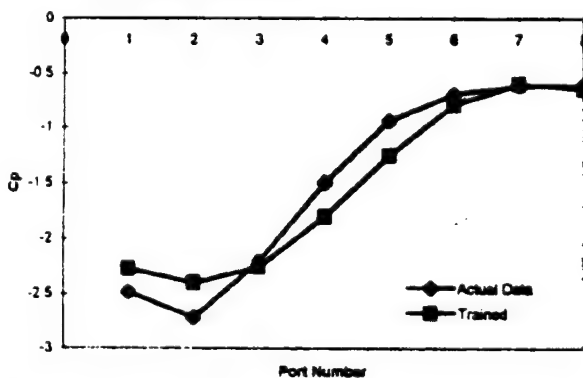


Fig. 27: Pressure distribution for Fig. 24 at time $t = 0.25s$.

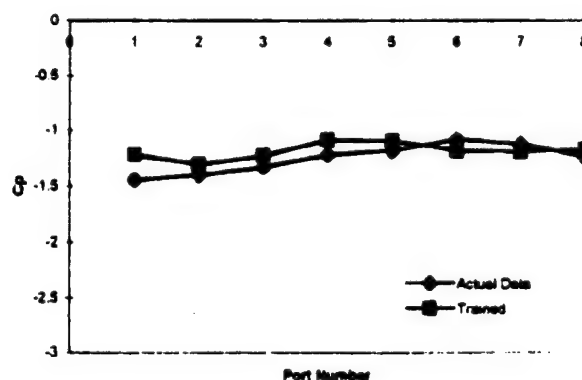


Fig. 28: Pressure distribution for Fig. 24 at time $t = 0.5s$.

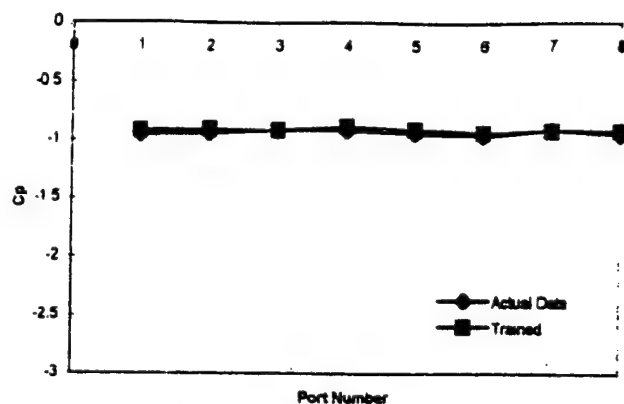


Fig. 29: Pressure distribution for Fig. 24 at time $t = 0.75s$.

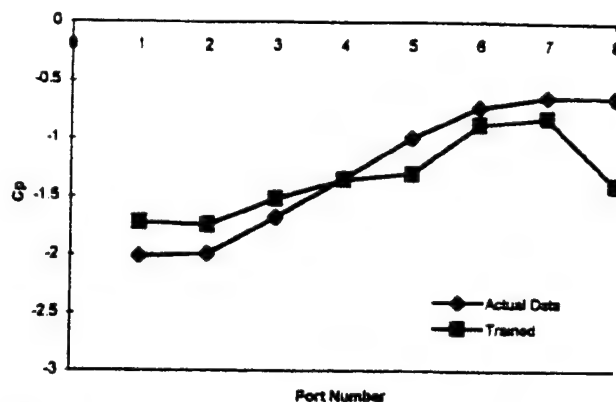


Fig. 30: Pressure distribution for Fig. 24 at time $t = 0.4s$. (Maximum error case)

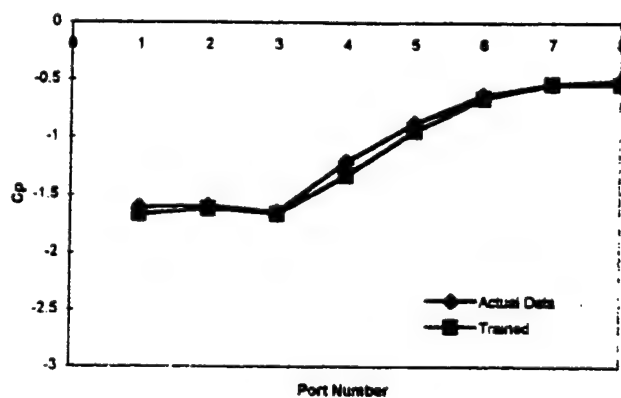


Fig. 31: Pressure distribution for Fig. 25 at time $t = 0s$.

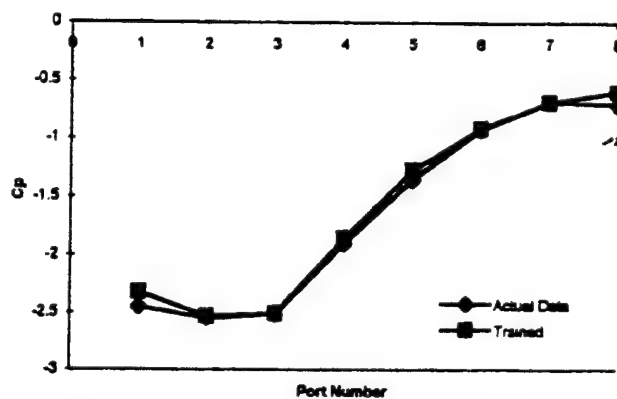


Fig. 32: Pressure distribution for Fig. 25 at time $t = 0.25s$.

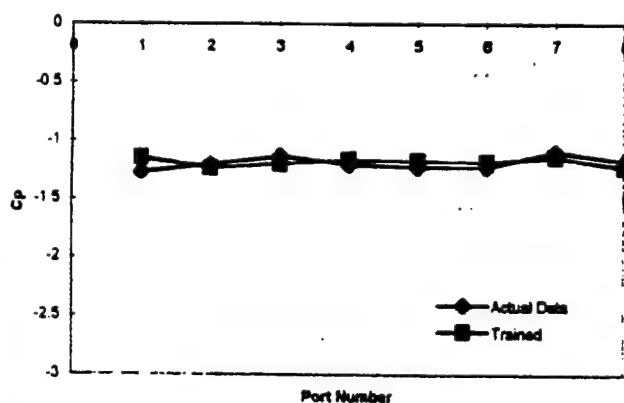


Fig. 33: Pressure distribution for Fig. 25 at time $t = 0.5s$.

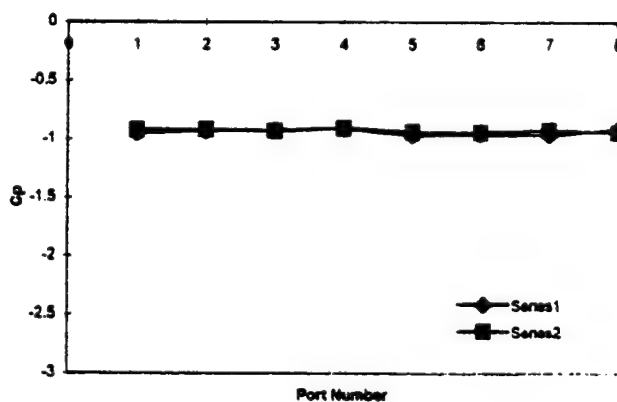


Fig. 34: Pressure distribution for Fig. 25 at time $t = 0.75s$.

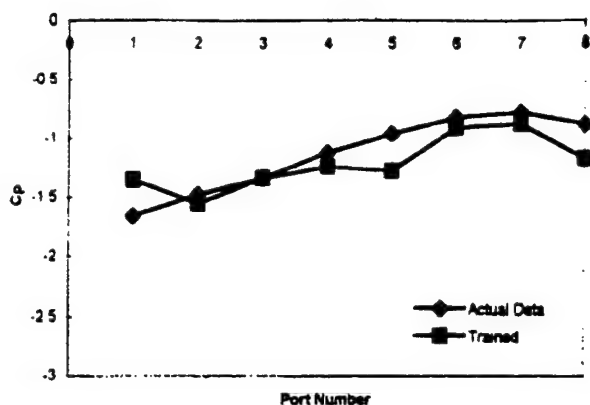


Fig. 35: Pressure distribution for Fig. 25 at time $t = 0.4s$.
(Maximum error case)

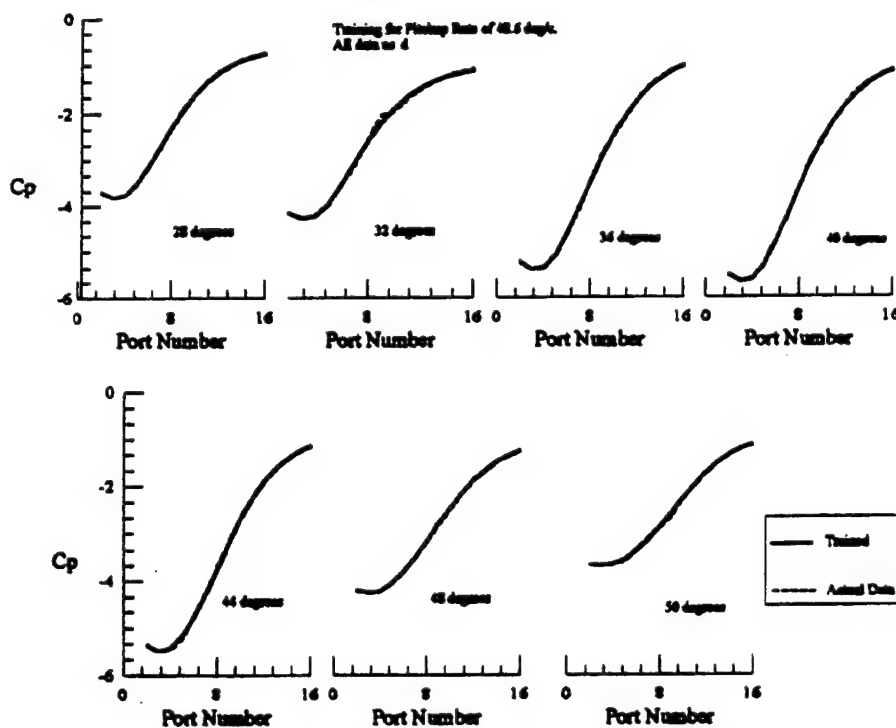


Fig. 36: Neural network predictions of pressure distributions for pitchup rate of $48.6^\circ/s$. Network was trained using all data from all pitchup rates

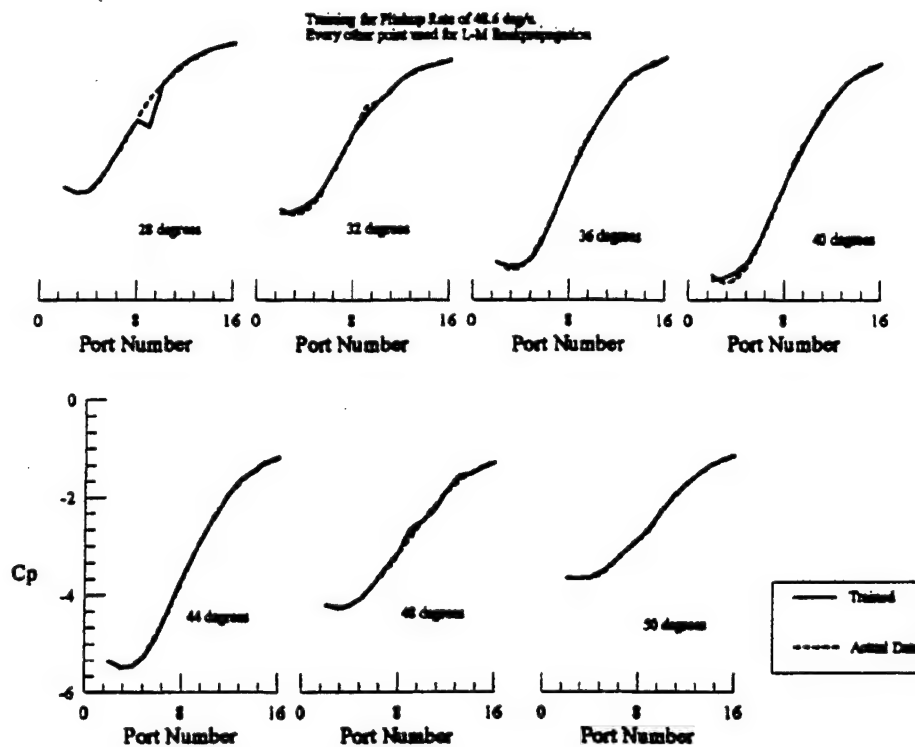


Fig. 37: Neural network predictions of pressure distributions for pitchup rate of 48.6°/s. Network was trained using every other point from full data set including data from all pitchup rates.

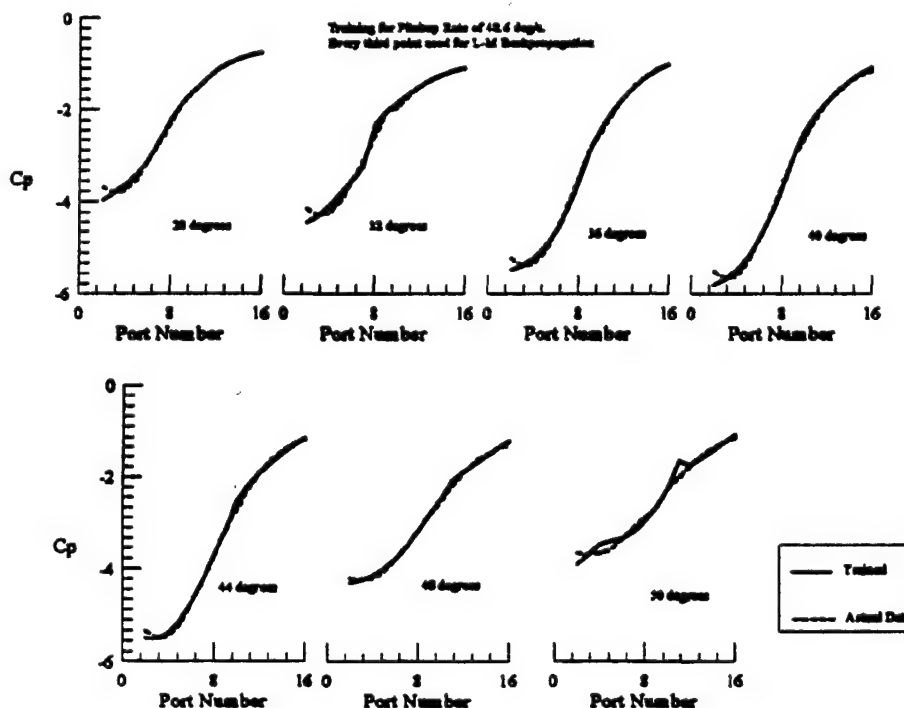


Fig. 38: Neural network predictions of pressure distributions for pitchup rate of 48.6°/s. Network was trained using every third point from full data set including data from all pitchup rates

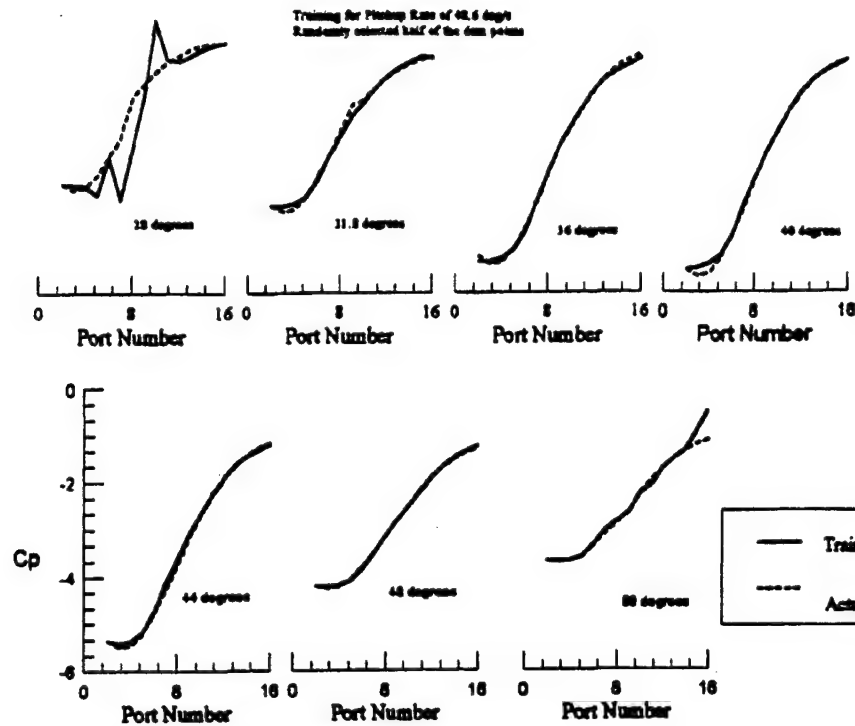


Fig 39: Neural network predictions of pressure distributions for pitchup rate of 48.6°/s. Network was trained using half of the data randomly chosen from the full data set.

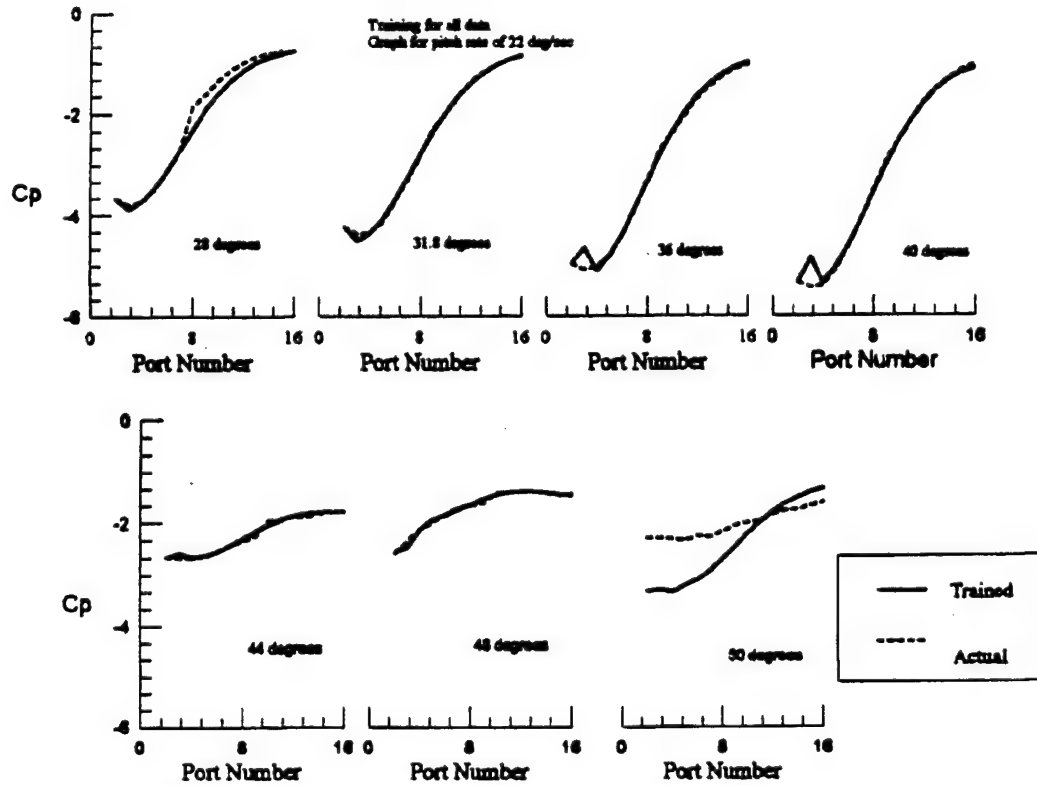
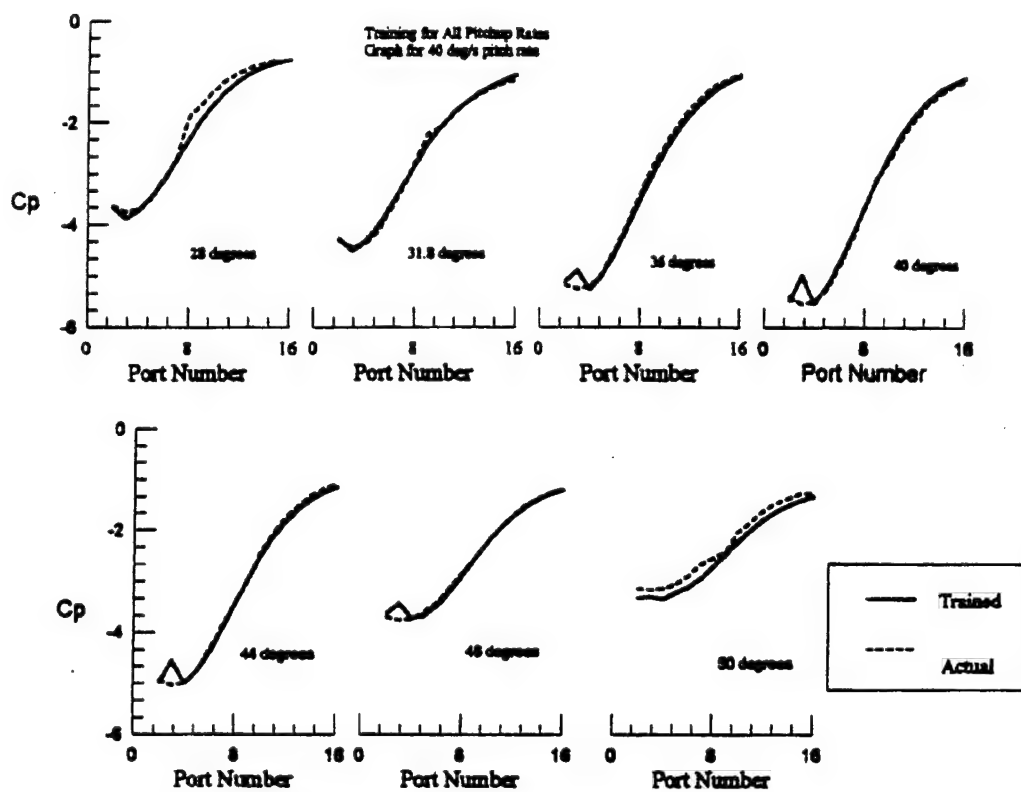


Fig. 40: Neural network predictions of pressure distributions for pitchup rate of 22°/s. Network was trained using half of the data randomly chosen from the full data set.



Graph for pitch rate of 40 deg/sec. Trained with half of all data / all rates.

Fig. 41: Neural network predictions of pressure distributions for pitchup rate of 40°/s. Network was trained using half of the data randomly chosen from the full data set.

Appendix III

FUZZY LOGIC IDENTIFICATION OF SHIP MOTIONS IN RESPONSE TO VARYING WAVE INCIDENCE

Christopher T. Moore and Demetri P. Telionis
Department of Engineering Science and Mechanics
Virginia Polytechnic Institute and State University
Blacksburg, VA 24061-0219

Abstract

A fuzzy logic identification code was prepared. The program was trained with experimental data of pitch and roll of a ship model at various incidences to oncoming waves. The program can then predict the response of the model to any wave and at any incidence.

1. Introduction

The skipper of a small sailing boat receives a variety of signals through his feeling of the heeling and pitching of his vessel, his feeling of accelerations in heeling, pitching and yawing, the feeling of sheet and tiller resistance, the observation of sail shape and tell tail direction and the shape and direction of the waves. In response to all these inputs and with very little brain action, he sustains a very delicate balance of various forces exerted on his vessel, maintains its stability and maximizes its performance.

It would be desirable for any naval vessel to be equipped with a central processing unit, say the "brain" of the vessel, that would receive signals from a variety of sensors and respond accordingly with controls that would produce the desired motion. More specifically, such a unit should be able to recognize quickly the characteristics of the sea surface, like direction, wavelength, etc. of all oncoming waves, wind direction and strength, predict the response of the vessel for the immediate future and activate the necessary controls to achieve a desired motion. With the speed and capacity of today's computers and the development of the theory of fuzzy logic systems

and artificial neural networks this is today well within reach.

Fuzzy logic and neural nets have been employed successfully so far as identifiers of dynamic flow phenomena. Schreck et al¹ demonstrated application in unsteady aerodynamics of system-identification and modern control methods based on the use of artificial neural networks (ANN). ANNs were shown to successfully model vortex dynamics principles^{1,2}. Further attempts were also reported later^{3,4}. Fuzzy logic systems (FLS) appear to be equally capable system identifiers. Comparisons of the two techniques^{4,5}, i.e., ANN versus FLS in different applications seem to favor the latter. However, we believe that neural networks and fuzzy logic have complementary strengths and a symbiotic relationship between the two holds the secret to effective system identification and control.

In this paper we report on the training of a fuzzy logic program in terms of data obtained in a towing tank. A ship model is allowed to respond to waves at various incidences. Its response to pitch and roll is recorded as well as the characteristics of the incident waves and the incidence angle. The model's response for arbitrary values of the parameters are then predicted.

2. Fuzzy-Logic Identifier & Controller

In a simplistic way, a fuzzy-logic system can be thought of as a black box that can be trained to provide certain outputs, if fed with certain inputs. This task of course can also be executed by any spline algorithm, or interpolating routine. However, fuzzy-logic

systems (FLS) can carry out such tasks faster, requiring much less computer space. Another great advantage of FLS is that they can be continuously upgraded simply by adding more data to an existing system or even adding new controlling variables. In simple terms, such systems "learn by experience." Moreover, they can admit as input, either crisp numerical data or fuzzy linguistic commands.

The fuzzy logic system used in this experiment is based on an optimized system as outlined by Wang⁴ for identifying non-linear systems in control applications. The program which was used has been under development with the goal of eventually controlling systems whose aerodynamic/hydrodynamic effects are too complex to model for classical control purposes. In its early stages of development, the program has been used successfully to fit complex curves based on partial data sets. It accepts as input the following data: A cluster radius for determining the complexity of the fuzzy rule base, a Gaussian membership function shape variable which determines the effect of a fuzzy rule on its surroundings, and the training input-output pairs.

The cluster radius determines the minimum amount that one point in the training data must differ from all other points in order to be part of a new fuzzy rule. The advantage of this clustering method is that for any given system and cluster radius there is a limit to the number of fuzzy rules which can be created. Thus the cluster radius directly determines the complexity of the fuzzy rule base for any given system. Here, the cluster radius was chosen so that each input-output pair created a new rule, thereby ensuring that the program would return accurate values at the original data points.

The Gaussian membership function shape variable has by far the most significant effect on the smoothing effect of the predictor program and therefore the most care must be taken in its specification. If the shape variable is too small, then all predicted values will take on the magnitude of the nearest fuzzy rule, resulting in large regions of like points. If, on the other hand, the shape variable is chosen too large, then a fuzzy rule will effect a large area of surrounding values, possibly including other rule supports or center values. This will result in very smooth but inaccurate results. It is, therefore, imperative that a reasonable compromise be determined between these conditions. For the purposes of this experiment, this compromise was found through trial and error, although it seems

likely that with a thorough knowledge of the input-output ranges and the cluster radius, a more rigorous method of determining this value should be possible.

3. Facilities, Instrumentation and Procedure

The Virginia Tech towing tank has a 4x6 ft cross section and is about 100 ft long. This tank is equipped with a wave making machine. Waves with different amplitudes and wavelengths were generated. Their characteristics were monitored by two free surface elevation sensors. A ship model was placed in the tank at various incidences to the oncoming waves as shown in Fig. 1. The model was mounted on the carriage by a mechanism that permits heave, pitch and roll but restrains and controls the angle of incidence. Linear transducers provide signals proportional to pitch and roll.

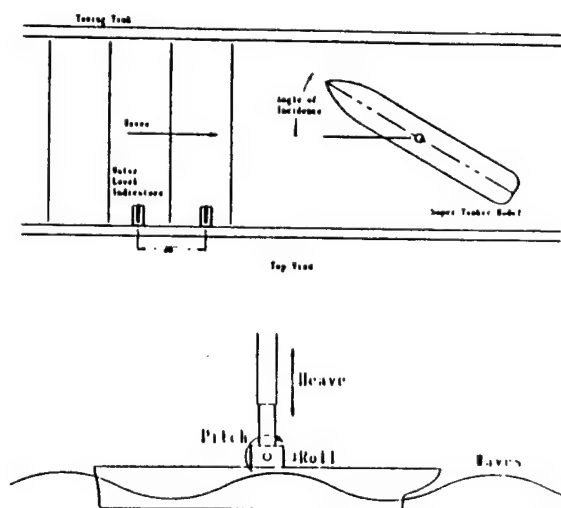


Fig. 1 Schematic of model mounted on a heave post that will allow pitch and roll through a gimballed tow point.

The fuzzy logic system was trained with data obtained with different wave characteristics and ship incidences. The idea was to train the artificial intelligence system to predict the response of the vessel, namely pitch and roll characteristics to new conditions. More specifically, the ship "learns" to recognize the condition of the sea it finds itself in. It then predicts how it will response, if it points in a different direction.

In order to test the ability of the fuzzy logic system to predict the dynamic response of the vessel to oncoming waves, it is first necessary to somehow quantify the waves themselves. In this experiment,

time records of the oncoming waves were recorded, using capacitance driven water level indicators, along with the responses of the vessel. By taking the data in this manner, we are able to post-process the time record to reveal magnitude or frequency data as necessary. Since the fuzzy logic system is capable of recognizing non-linear relationships between the inputs and outputs of the system, it was decided to attempt to train the system using the angle of incidence, wave magnitude, wave frequency, and wave height as common inputs. In addition, when trying to predict the roll position of the vessel, the pitch was used as an additional input and vice versa.

The data taken for this experiment consisted of 13 angles of incidence ranging from -30° to 30° in 5° increments. The incident waves were generated at three different magnitudes at 0.25 Hz and 0.5 Hz for a total of 78 different data sets. Each data set in turn contained time records of two water level transducers separated by 21", the roll angle of the ship, and the pitch angle of the ship. Each time record was 10 seconds long and was sampled at 100 Hz. Unfortunately, it was determined after the data had been taken that the largest magnitude wave at 0.5 Hz was affected by some sort of mechanical interference and thus had to be removed from the training set.

4. Results, Conclusions & Recommendations

To test the code, a case for intermediate values of the parameters was predicted. At these values of the parameters data were also obtained which were not employed in the training of the fuzzy-logic system. In this way it was possible to compare directly the predicted behavior against experimental data.

Typical results are presented in Figs. 2 and 3 for roll and pitch respectively, for an incidence of 15° at a wave frequency of 0.5 Hz. The phase and frequency of the response of the model are predicted reasonably well. However, the waveform contains higher harmonics which are not present in the actual data.

These results are preliminary in nature and are not satisfactory at present. Much better predictions were achieved earlier for other experimental data. Apparently ship motions are highly nonlinear and may require more input parameters in order to facilitate more accurate predictions.

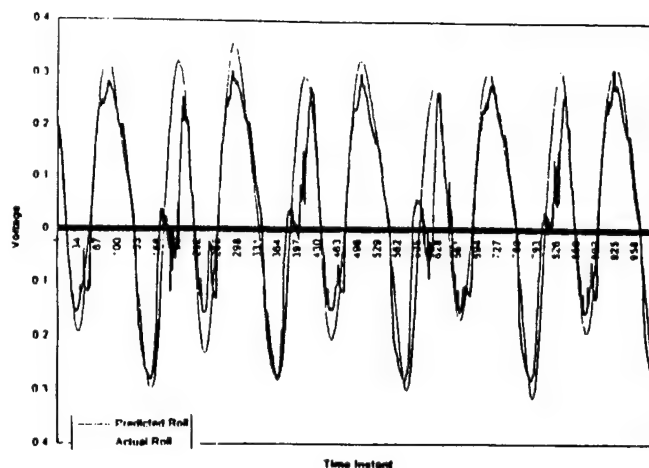


Fig. 2 Predicted and actual roll of the model at a wave incidence of 15° and a frequency of 0.5 Hz.

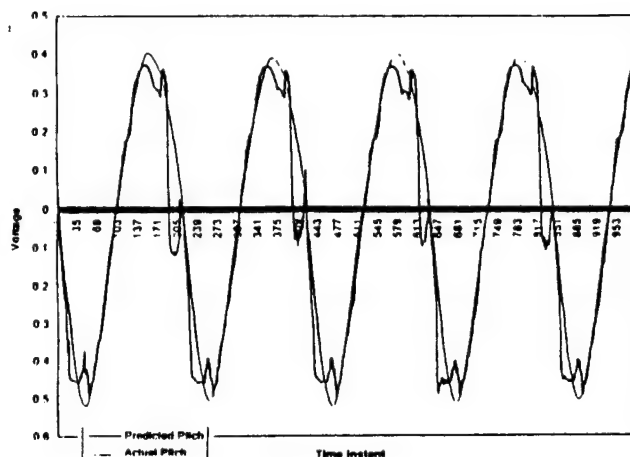


Fig. 3 Predicted and actual pitch of the model at an incidence of 15° and a frequency of 0.5 Hz.

Fuzzy-logic systems could also be trained to control motions⁶. To this end, data must be collected on the response of a body to the deployment of control hardware. Consider again, for example, a model vessel equipped with two fins which could be activated to control its roll. Different amplitudes and frequency motions of the fins are generated and the response of the vessel is monitored via its sensors. These prescribed tests are repeated with the vessel placed in a wavy sea and again the data are employed to train the FLS. The system now can be used to predict the characteristics of deployment necessary to achieve a certain motion. This is a theoretical exercise but its im-

plementation is straightforward although a little more involved.

The FLS controller decides what level of deployment is necessary to achieve the desired motion in the specific environment. For example, what angle of fin action is needed for the specific waves the vessel is encountering. The controller then activates the control hardware. The FLS continuously samples its sensors to follow up the motion and compares its progress with its predicted motion. It corrects in real time for small perceived discrepancies and uses this new information to improve its "understanding" i.e., to further train itself.

This effort is continued and the authors will report subsequent results in future publications.

References

1. Schreck, S. J., Faller, W. E., and Luttgies, M. W., "Neural Network Predictions of Three-Dimensional Unsteady Separated Flow Fields," AIAA Paper No. 93-3426-CP, Monterey, CA, August 1993.
2. Faller, W. E., Schreck, S. I., Luttgies, M. W., "Real-Time Prediction and Control of Three-Dimensional Unsteady Separated Flow Fields Using Neural Networks," AIAA Paper No. 94-0532, Reno, Nevada, Jan. 1994.
3. Steck, J. E., and Roshsat, K., "Use of Neural Networks in Control of High Alpha Maneuvers," AIAA Paper No. 92-0048, Reno, NV, Jan. 1992.
4. Wang, Li-Xin, "Adaptive Fuzzy Systems and Control, Design and Stability Analysis," Prentice Hall, New Jersey, 1994.
5. Kosko, Bart, "Neural Networks and Fuzzy Systems," Prentice Hall, New Jersey, 1992.
6. Husson, D., "The Design of the Charles-de-Gaulle," Carénes, April, 1955.

A Fuzzy Controller for High-Alpha Delta Wing Maneuvers with Deployable Control Surfaces

Othon K. Rediniotis[†], Norman W. Schaeffler* and Demetri P. Telionis^{††}
Virginia Polytechnic Institute and State University
Blacksburg, Virginia

Abstract

Fuzzy logic system-identification and control techniques are employed in high-alpha delta-wing unsteady aerodynamics. A cavity-flap equipped delta wing is executing pitch-up maneuvers while the cavity flaps are dynamically employed aiming to modify and control the behavior of the two leading-edge vortical structures and thusly their effect on the pressure distribution and aerodynamic loading of the wing. First a fuzzy identifier is constructed to predict the temporal evolution of the leeward pressure distribution and the aerodynamic loads for given time histories of pitching, $\alpha(t)$, $\dot{\alpha}(t)$ and flap deployment $\phi(t)$, $\dot{\phi}(t)$. Then, a fuzzy controller is devised which, for defined $\alpha(t)$, $\dot{\alpha}(t)$ yields the cavity-flap deployment schedule $\phi(t)$, $\dot{\phi}(t)$ so that a desired time history of L/D is achieved.

Introduction

The aerodynamics of supermaneuver-performing aircraft has been a great challenge to aerodynamicists but still many questions in this area are unanswered. This is partly due to shortage of wind-tunnel hardware able to simulate complex supermaneuvers of sensor-instrumented models and allow the measurement of the properties of the model-flowfield interaction. Moreover, when the control of these interactions becomes our objective, the task becomes understandably overwhelming: different flow-control devices have to be tested, each one at several different dynamic deployment schedules and rates, as well as testing of combinations of flow-control devices. When a sufficiently large data bank of these test data is generated, then the daunting question emerges: How is all this information efficiently implemented into the next generation super-agile aircraft? Since the rapid rates of motion during a supermaneuver are beyond the pilot's response limits, an active controller between the pilot and the aircraft is necessary. To reinforce the gravity of the problem along comes the inadequacy of the conventional adaptive control schemes: the high rates and large motion

[†] Assistant Professor, Member AIAA

* Research Assistant

^{††} Professor, Member AIAA

amplitudes involved in a supermaneuver preclude the local linearization of the strongly nonlinear governing equations.

The application in unsteady aerodynamics of system-identification and modern control methods based on the use of artificial neural networks (ANN) have been recently investigated¹⁻³. There¹, ANNs were shown to successfully model vortex dynamics principles. However, further attempts to implement neural network controllers³ did not seem to provide sufficient accuracy. Similar occurrences in other fields⁴ have cost ANN popularity some loses. In fact, as discussed later, fuzzy logic systems (FLS) seem to be partly profiting from these ANN loses. Comparisons of the two techniques^{4,5}, i.e., ANN versus FLS in different applications seem to favor the latter. However, we believe that neural networks and fuzzy logic have complementary strengths and a symbiotic relationship between the two holds the secret to effective system identification and control.

In this paper we first demonstrate that fuzzy logic methods can successfully identify nonlinear aerodynamic systems. Our system consists of a pitching delta wing with dynamically deployed cavity flaps during the maneuver. We identify the effect this system has on the temporal evolution of the leeward-side pressure distribution as well as the aerodynamic loads. Once a system model has been generated, a fuzzy controller is constructed with the objective to control the cavity-flap deployment schedule during pitch-up, so that a certain optimization criterion is satisfied, for example, the maximizing of the ratio L/D (lift over drag) for all times during the maneuver.

Facilities and Instrumentation

The present research is being conducted in the VPI & SU Stability Wind Tunnel. This Tunnel has a 6' x 6' test section and an excellent quality of flow. The tunnel has been recently equipped with a dynamic strut which was given the acronym DyPPiR for "Dynamic-Plunge-Pitch-Roll" mechanism. The design, construction and calibration of this facility involved many faculty at VPI & SU, under the direction of Dr. Roger Simpson and five years of

intensive work. A discussion of the main elements of the design can be found in Ref. 6 and the accompanying instrumentation in Ref. 7.

The DyPPiR can provide simultaneous plunging, pitching and rolling of models on the order of 100 lb in weight, at a frequency of up to 10 Hz, depending on the amplitude of the motion. These motions can be independently controlled by software. Any combination of arbitrary motions is possible. In this case, pitch up motions are executed. Such motions have been tested earlier in two much smaller facilities^{8,9}, a wind tunnel and a water tunnel and at Reynolds numbers of the order of 10^4 . Simultaneous plunging of the DyPPiR carriage and pitching of the pitch actuator induces pitching of the model about its quarter-chord axis. The aim here is to control the leading edge vortices and delay breakdown, while pitching up to high angles of attack. This is pursued by deploying cavity flaps.

In the present experiments we employ a $2' \times 3'$ delta wing model (Fig. 1) which has been tested extensively in this facility in steady flow⁷. The model is hollow to provide space for instrumentation. The top surface of the model is equipped with three rows of pressure taps. Pressure transducers are positioned beneath the instrumented surface to provide unsteady pressures with a high frequency response. A 32-transducer Electronic Pressure Scanner (ESP) from PSI, Inc. with a pressure full scale of ± 20 in H_2O was employed. The ESP Pressure Scanner was interfaced with a laboratory computer and was on-line calibrated through instrumentation by AEROPROBE Corp. The system consists of an ESP interface/data-acquisition board PDA-3101 (31 KHz max sampling rate) and an ACCUPRES computer-controlled, on-line pressure calibrator. Figures 2(a) and 2(b) present the coordinate systems used and the pressure port distribution, respectively.

Figure 3 presents the carriage actuators, sting and delta-wing model as seen from upstream. A view of the same setup from downstream is shown in Figure 4. A six-component dynamic balance was employed to measure the aerodynamic loads.

Fuzzy Logic Systems (FLS)

A recently developed field in mathematics, the theory of fuzzy sets and the logic stem-

ming from it have been attracting attention, sometimes at the expense of ANN popularity. In fact, in the semiconductor industry, microcontroller pundits predict that semiconductor-based fuzzy technology will be as prevalent in products by the end of the decade as microprocessor technology is today. Although, traditionally, fuzzy logic has been viewed as a technique for representing imprecise, ambiguous and vague information, nothing prevents it from successfully dealing with concrete, quantitative and precise data. In fact, the Universal Approximation Theorem proves that fuzzy logic systems are capable of uniformly approximating any nonlinear function to any degree of accuracy.

Figure 5 presents a schematic of the basic configuration of the fuzzy logic systems proposed in this work. The fuzzy rule base consists of a collection of fuzzy if-then rules in the following form:

$$R^{(\ell)} : \text{If } x_1 \text{ is } F_1^\ell \text{ and } \dots \text{ and } x_n \text{ is } F_n^\ell, \text{ THEN } y \text{ is } G^\ell, \quad (1)$$

where F_i^ℓ and G^ℓ are fuzzy sets,

$\underline{x} = (x_1, \dots, x_n)^T$, y are the input and output linguistic variables, respectively, and $\ell = 1, \dots, M$ with M being the number of rules.

However, in engineering systems inputs and outputs are real-valued variables in crisp sets and not linguistic variables in fuzzy sets. The conversion from the former to the latter and vice-versa is achieved through the fuzzifier and defuzzifier respectively. The fuzzy inference engine is the heart of the system and maps the fuzzy inputs to the fuzzy outputs properly employing the rules from the fuzzy rule base. In one of our approaches we use center average defuzzifier, product-inference rule, singleton fuzzifier and Gaussian membership function. Then the fuzzy system reduces to:

$$F(\underline{x}) = \frac{\sum_{\ell=1}^M y^\ell \left[\prod_{i=1}^n a_i^\ell \exp \left(- \left(\frac{x_i - \underline{x}_i^\ell}{\sigma_i^\ell} \right)^2 \right) \right]}{\sum_{\ell=1}^M \left[\prod_{i=1}^n a_i^\ell \exp \left(- \left(\frac{x_i - \underline{x}_i^\ell}{\sigma_i^\ell} \right)^2 \right) \right]} \quad (2)$$

where $\underline{x} = (x_1 \dots, x_n)^T \in U$ (U is the universe of discourse) is the input vector, n is the number of antecedents (inputs) and M is the number of rules. \underline{x}_i^ℓ , σ_i^ℓ , a_i^ℓ are the parameters of the

Gaussian membership functions and \underline{y}^ℓ are the centers of the output fuzzy sets. Although our techniques are capable of identifying multi-input, multi-output systems, here to facilitate the reader's understanding, a multi-input, single-output system is presented. We state here the following Universal Approximation Theorem⁴:

For any given real and continuous function G on a compact set $U \in \mathbb{R}^n$ and arbitrary $\epsilon > 0$ there exists a fuzzy logic system F in the form of Eq. (2) such that

$$\sup_{\underline{x} \in U} |F(\underline{x}) - G(\underline{x})| \leq \epsilon. \quad (3)$$

Generating rules and membership functions for fuzzy logic is essentially a learning process. Here is where the utilization of neural network techniques enters our modeling process. Using supervised learning, a neural network can generate or sort out rules and tune the membership function parameters. For instance, for the single-output system (2) training is achieved using a back-propagation algorithm to determine the parameters \underline{x}_i^ℓ , σ_i^ℓ , \underline{y}^ℓ (without loss of generality the a_i^ℓ 's are set equal to 1).

Sample Results and Discussion

System Identification

We first explore the capabilities of fuzzy logic systems to model the dynamic evolution of the pressure distribution on the leeward side of the model. The 75°-sweep delta wing was pitched from $\alpha = 28^\circ$ to $\alpha = 43^\circ$ with several different time histories of $\alpha(t)$ and $\dot{\alpha}(t)$. During this maneuver the two cavity flaps were deployed from $\phi = 0^\circ$ to $\phi = 30^\circ$ (Figure 6) with several different deployment schedules $\phi(t)$ and $\dot{\phi}(t)$, and for each of these experiments the pressure distribution was captured at 900 time instances during the pitch-up. Each experiment was repeated 20 times and the pressure data were ensemble-averaged.

From all the collected pressure data a data bank was formed and was subsequently used to generate the fuzzy identifier. Our objective was to devise an identifier like the one shown in Fig. 7 which, given the time histories, $\alpha(t)$, $\dot{\alpha}(t)$, $\phi(t)$, $\dot{\phi}(t)$ and the pressure distribution

at $t = 0$ would be able to predict the entire temporal evolution of the pressure distribution during the dynamic maneuver.

We developed an algorithm in C++ that implements a fuzzy rule base for any n -input, m -output system. The number of fuzzy regions per domain of antecedent and consequent is adjustable and so is the choice of membership function. In our first trials we used triangular membership functions. However, at latter effort, gaussian membership functions were found to work better. In results presented here we use the latter approach. The rules are generated initially from a set of input-output pairs. Each rule is assigned a degree equal to the product of the membership values of the antecedents and consequent. A rule is stored in the rule base only if a similar rule with higher degree does not already exist. That minimizes the number of rules, and makes the defuzzifying process faster.

Figure 9 presents the comparison between the predicted and the actual pressure distribution for the case $\phi(t) = \text{const} = 0$, $\dot{\phi}(t) = 0$ (flaps not deployed) and for the $\alpha(t)$ shown in figure 8 with $\dot{\alpha}(t) = 0.38$ rad/sec. The figure presents the pressure distribution along a cross-flow pressure port line (upper row in figure 2(b)), at different time instants during the maneuver, or equivalently, at different angles of attack. Only half of these data, arbitrarily chosen, were used in the fuzzy rule base generation. Nevertheless, the prediction is excellent for the entire data set.

Figure 10 presents the pressure distribution (predicted and actual) along the same pressure port line in different conditions, i.e., $\phi(t) = \text{const} = 30^\circ$, $\dot{\phi}(t) = 0$ (flaps deployed) for the $\alpha(t)$ shown in Fig. 8 and $\dot{\alpha}(t) = 0.38$ rad/sec.

The same fuzzy identifier is also employed to predict the integrated effect of the pressure distribution, i.e., the aerodynamic loads L (lift), D (drag), $M_{c/4}$ (quarter chord pitching moment).

In the final version of the paper, comparison between the predicted and the actual $C_p(t)$, $L(t)$, $D(t)$, $M_{c/4}(t)$ will be presented for several combinations of time histories $\alpha(t)$, $\dot{\alpha}(t)$, $\phi(t)$, $\dot{\phi}(t)$.

Fuzzy Controller

In the second part of this work the accumulated experimental data base is used to construct the fuzzy controller shown in Figure 11: for defined histories of $\alpha(t)$ and $\dot{\alpha}(t)$ the controller has to yield the cavity flap deployment schedule $\phi(t)$, $\dot{\phi}(t)$ so that a desired time history of the ratio $\frac{L}{D}(t)$ is achieved. It is obvious that the desired $\frac{L}{D}$ time history has to be within the limits of the aerodynamic effectiveness of the cavity flaps.

The pressure contour plots shown in Fig. 12 demonstrate the effect the cavity flaps have on the leeward-side pressure distribution along a cross-flow pressure port line (upper row in figure 2(b)). The image shows the evolution of the surface pressure as a function of angle of attack, or as a function of time. The fact that the pressure coefficient in the "without flaps" case has peaked and is beginning to decay is shown as the "island" of red in the upper left hand corner. In the "with flaps" case, the two yellow sections show evidence of merging and a new peak is just beginning to form as the motion ends.

From the above it is evident that in order to achieve high suction and therefore high lift values, throughout the entire maneuver, a composite cavity flap actuation schedule has to be employed. This schedule should involve none or low flap deflection at moderate angles of attack and full actuation at high angles where, as shown in Fig. 12, the flaps have their maximum effect in improving the suction. The fuzzy controller's objective is to determine this optimum schedule. The final version of the paper will present such optimum actuation schedules and their effect on pressure distribution and aerodynamic loading for several different histories of $\alpha(t)$, $\dot{\alpha}(t)$.

Our fuzzy controller has the following major advantage: it is expandable. This means that as more experimental data become available it can be used to expand the controller's fuzzy rule base. Thus, additional cavity-flap data could be used to improve the controller's

accuracy while data from experiments testing different control surfaces, or devices, such as apex flaps or leading-edge blowing could be used to expand the controller's capabilities.

However, the more complex the controller becomes the larger the number of fuzzy rules. It could easily reach the order of hundreds or thousands. This, in turn, means that, in order to implement a real-time controller for a maneuvering delta wing with several different control devices, the speed of 32-bit processors does not suffice, even when as few as 50 control action. More than one fuzzy coprocessor could be parallelly implemented to expand the system. This is why we are currently hardware implementing a dedicated fuzzy controller based on the VY86C570 12-bit FCA fuzzy coprocessor. Its inference speed is 10 times that of the conventional 32-bit processors.

Acknowledgements

This work was supported by the Air Force Office of Scientific Research, Project No. AFOSR-91-0310 and AASERT Project No. F49620-93-1-0455 and was monitored by Major Daniel Fant.

References

1. Schreck, S. J., Faller, W. E., and Luttgies, M. W., "Neural Network Prediction of Three-Dimensional Unsteady Separated Flow Fields," AIAA Paper No. 93-3426-CP, Monterey, CA, August 1993.
2. Faller, W. E., Schreck, S. I., Luttgies, M. W., "Real-Time Prediction and Control of Three-Dimensional Unsteady Separated Flow Fields Using Neural Networks," AIAA Paper No. 94-0532, Reno, Nevada, Jan. 1994.
3. Steck, J. E., and Roshsat, K., "Use of Neural Networks in Control of High Alpha Maneuvers," AIAA Paper No. 92-0048, Reno, NV, Jan 1992.
4. Wang, Li-Xin, "Adaptive Fuzzy Systems and Control, Design and Stability Analysis," Prentice Hall, New Jersey, 1994.
5. Kosko, Bart, "Neural Networks and Fuzzy Systems," Prentice Hall, New Jersey, 1992.
6. Ahn, S., Choi, K.-Y., and Simpson, R. L., "The Design and Development of a Dynamic Plunge-Pitch-Roll Model Mount," AIAA Paper No. 89-0048, 1989.
7. Rediniotis, O. K., Hoang, N. T., and Telionis, D. P., "Multisensor Investigations of Delta Wing High-Alpha Aerodynamics," AIAA Paper No. 91-0735, 1991.
8. Rediniotis, O. K., Klute, S. M., Hoang, N. T., and Telionis, D. P., 1992, "Pitch Up Motions of Delta Wings," AIAA Paper No. 92-0278, 1992, also *AIAA Journal*, in press.
9. Hoang, N. T., Rediniotis, O. K., and Telionis, D. P., "Three-D LDV Measurements Over a Delta Wing in Pitch-Up Motion," AIAA Paper No. 93-0185, 1993.

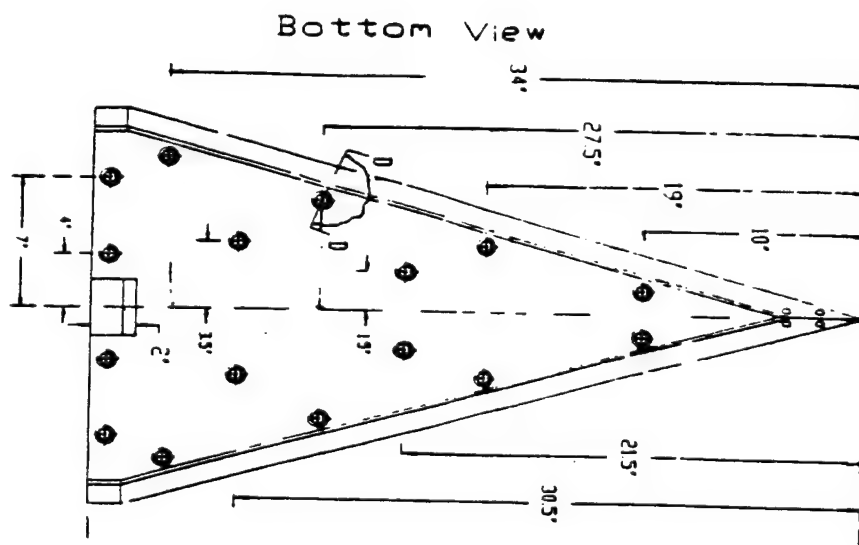
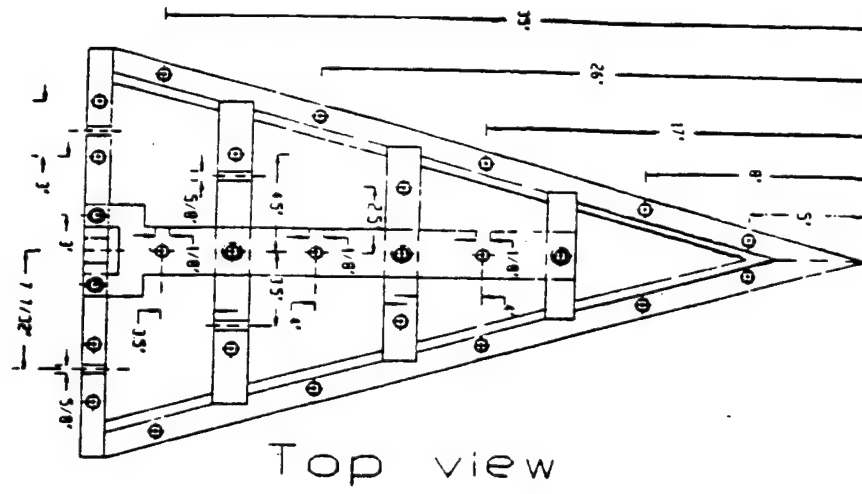
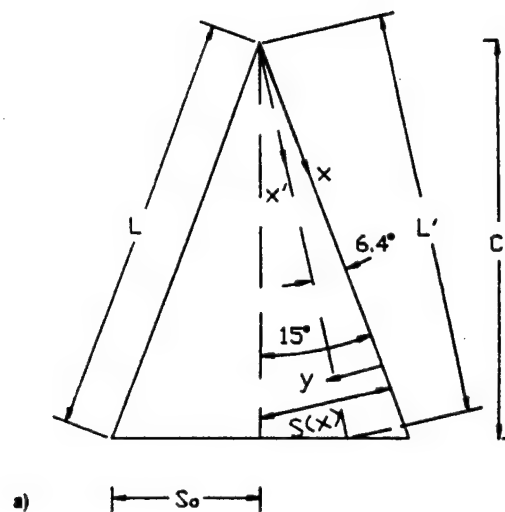
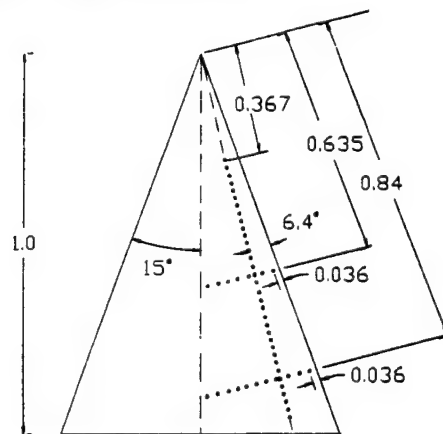


Fig. 1 The delta wing model.



Distances nondimensionalized
with respect to chord



Nondimensional pressure
b) port separation : 0.0183

Fig. 2 Coordinate systems used for the pressure data and pressure port distribution on the leeward side of the model; all dimensions are reduced by the chord length C .



Fig. 3 The carriage, acutators, sting and model as seen from upstream.

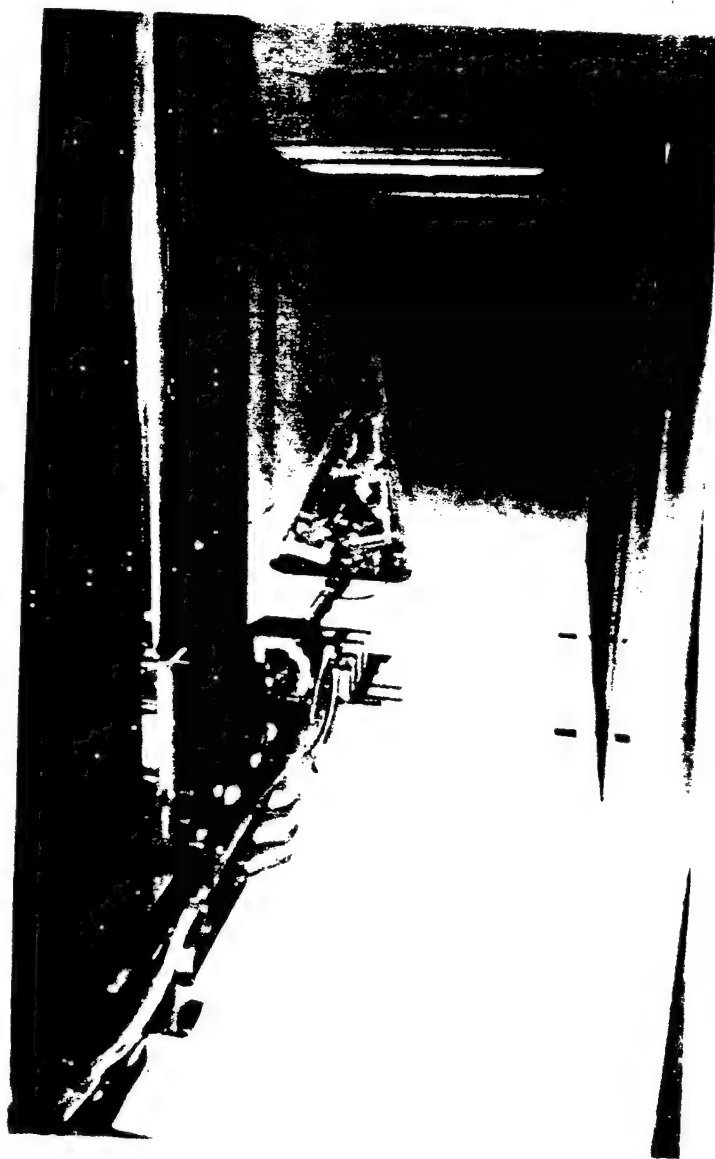


Fig. 4 The setup of figure 3 in a view from downstream.

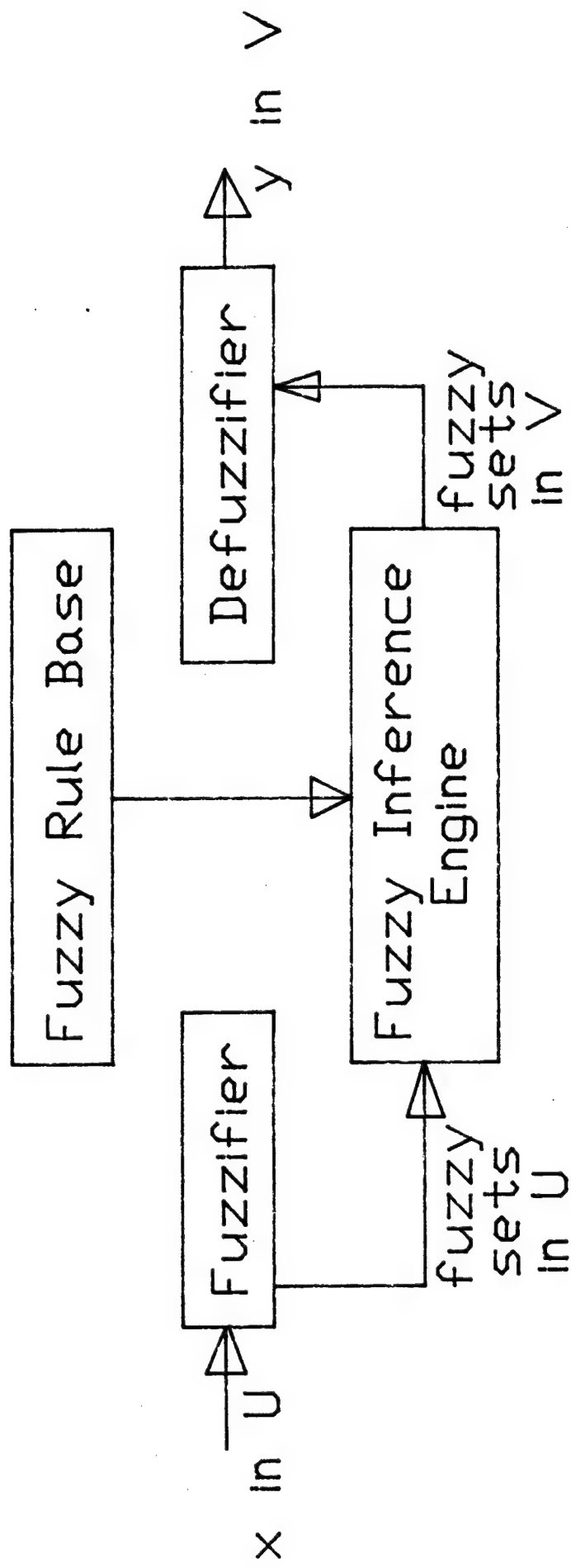


Fig. 5 The basic configuration of our fuzzy logic system.

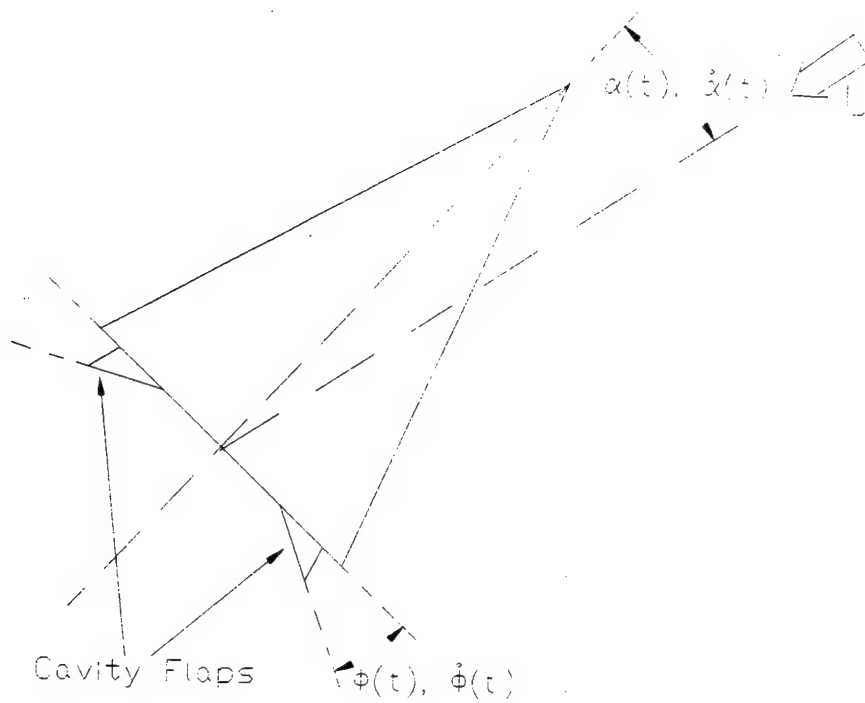


Fig. 6 Delta wing - cavity flaps configuration.

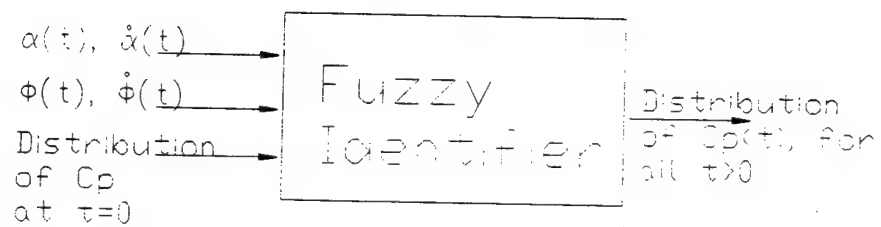


Fig. 7 The fuzzy system identifier.

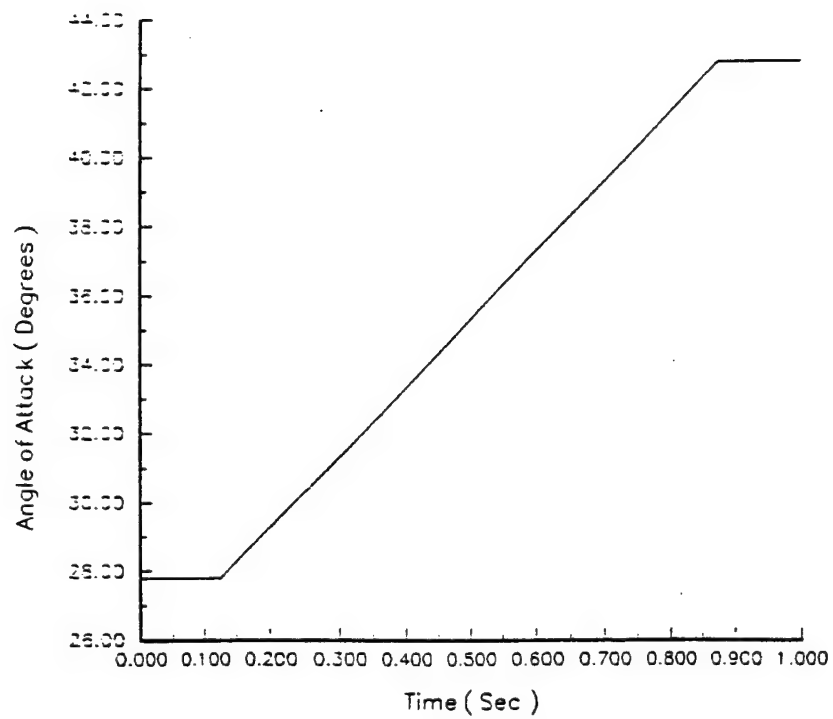
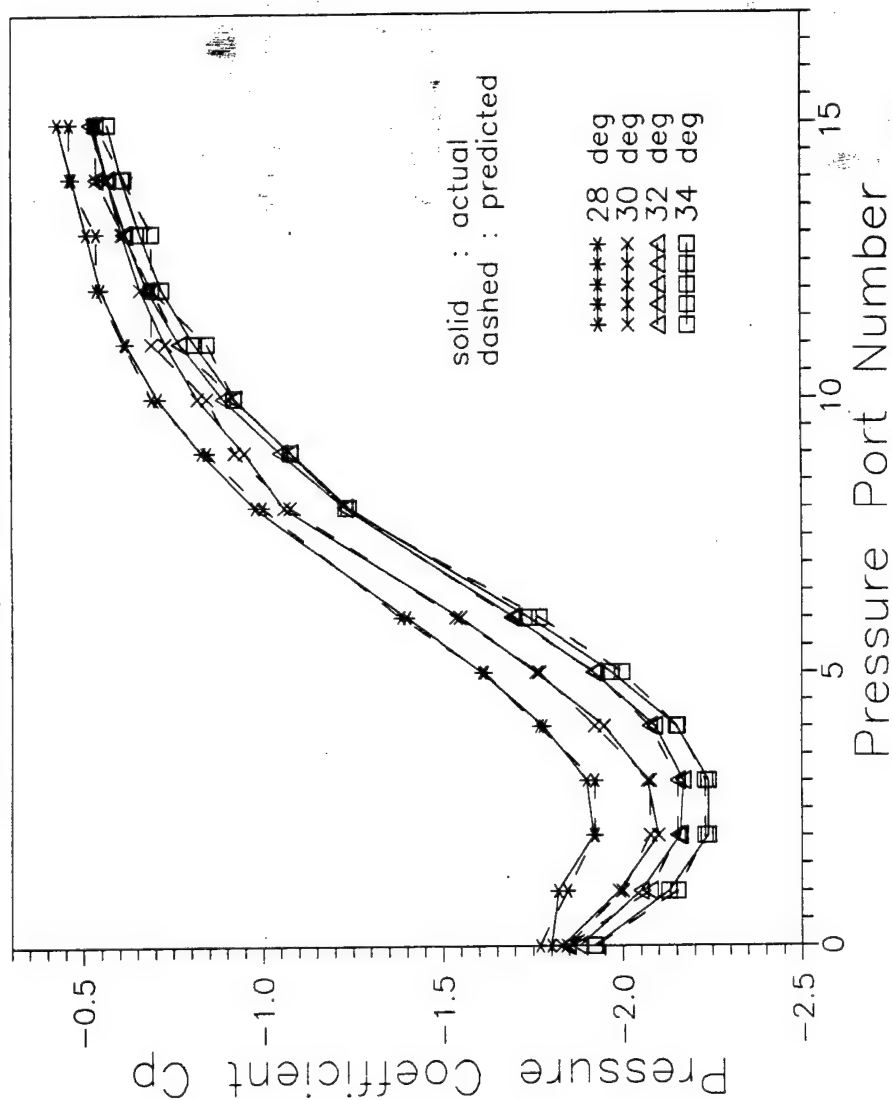


Fig. 8 Delta wing pitchup schedule.

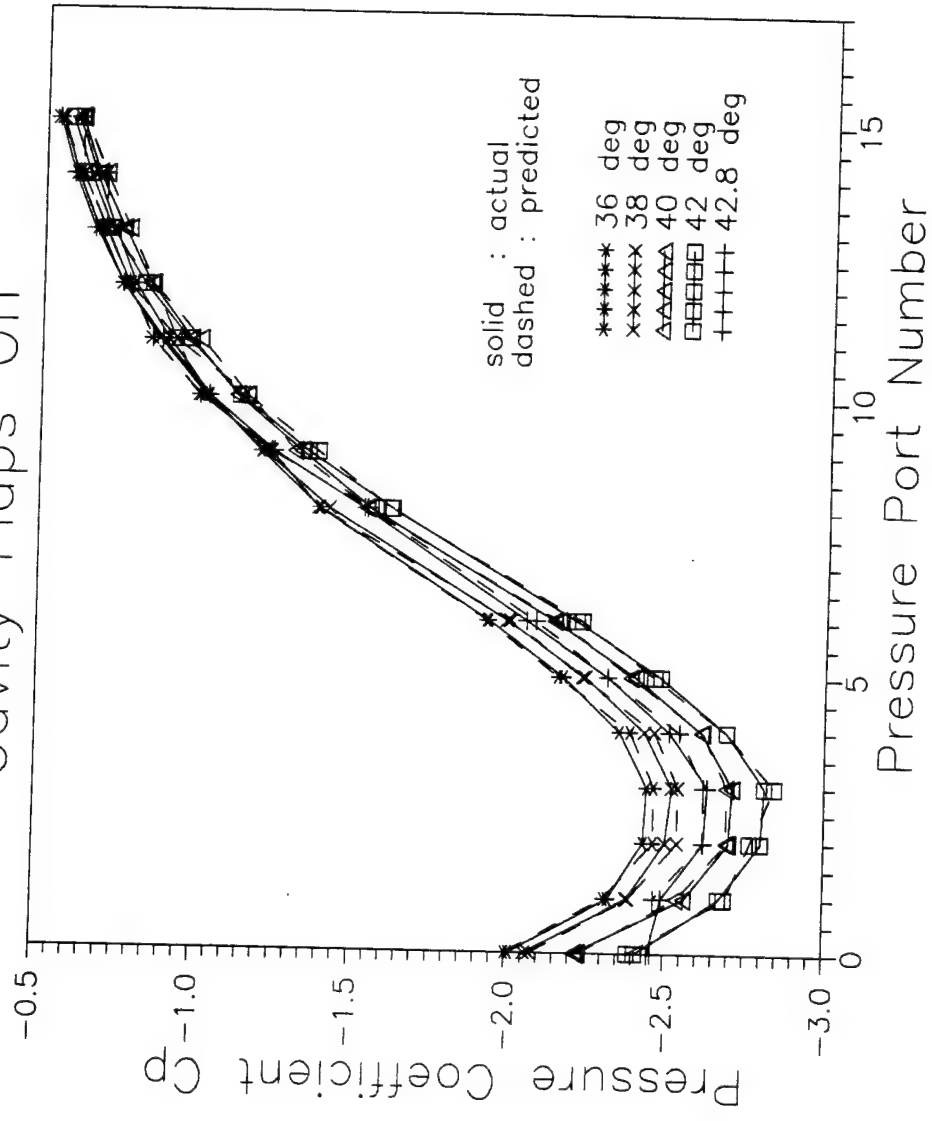
Cavity Flaps Off



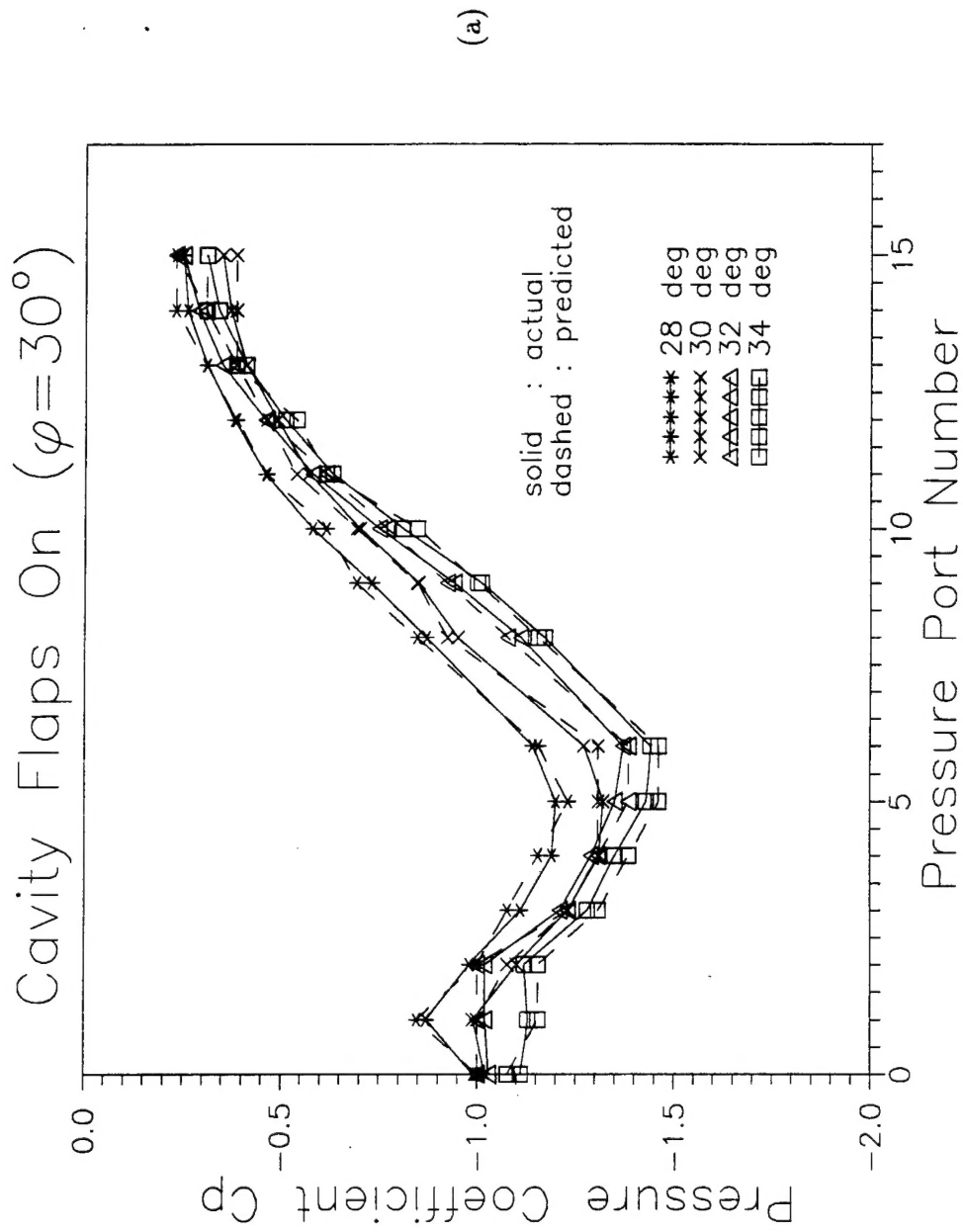
(a)

Fig. 9 Fuzzy identifier prediction for cavity flaps off: (a) $\alpha = 28^\circ$ to $\alpha = 34^\circ$ (b) $\alpha = 36^\circ$ to $\alpha = 42.8^\circ$.

Cavity Flaps Off

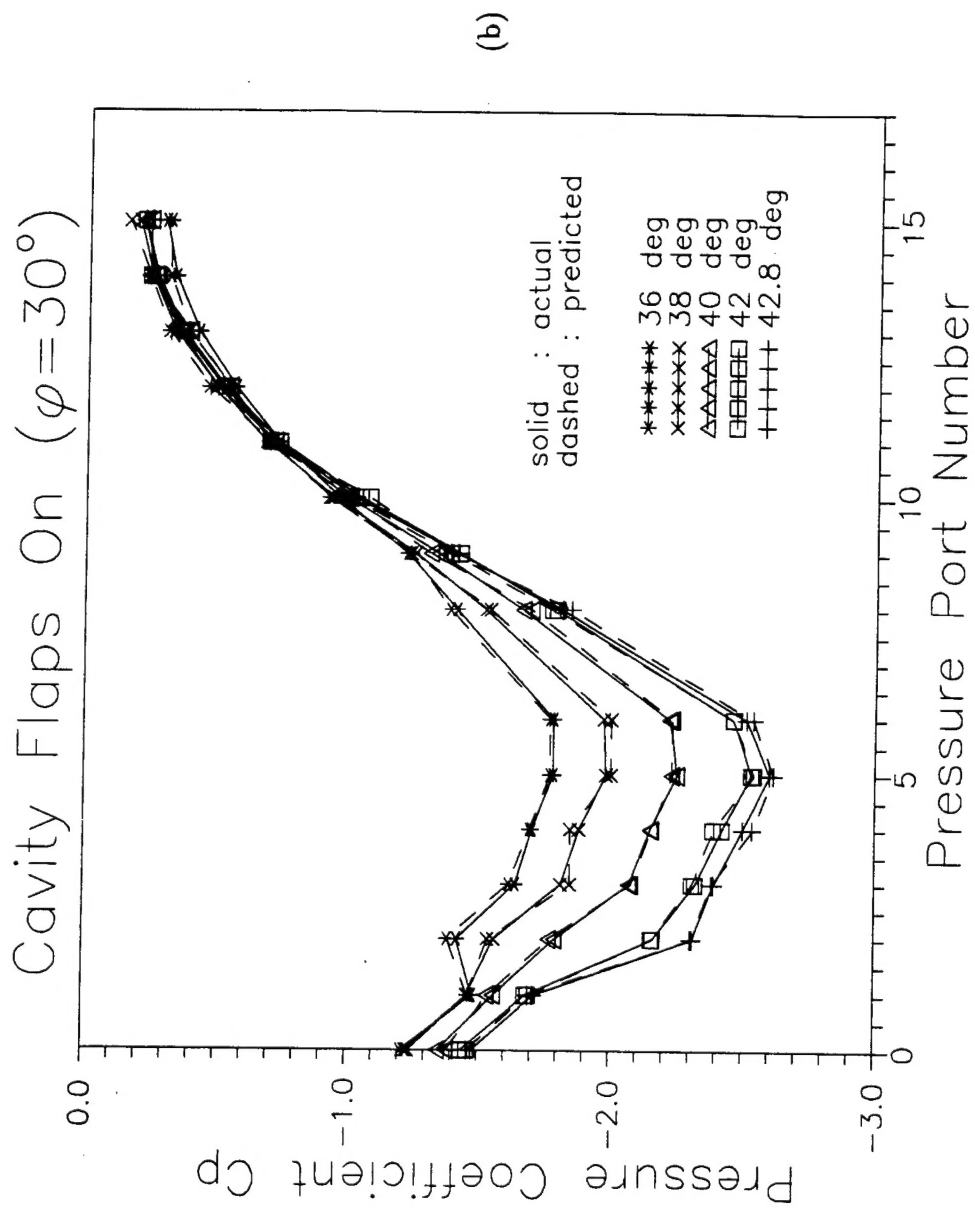


(b)



(a)

Fig. 10 Fuzzy identifier prediction for cavity flaps on ($\phi = 30^\circ$): (a) $\alpha = 28^\circ$ to $\alpha = 34^\circ$ (b) $\alpha = 36^\circ$ to $\alpha = 42.8^\circ$.



(b)

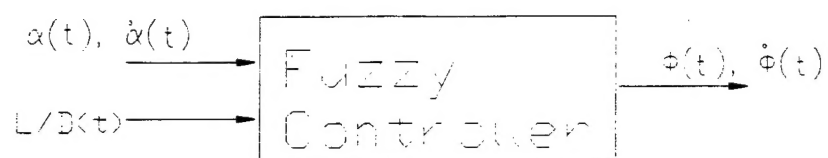
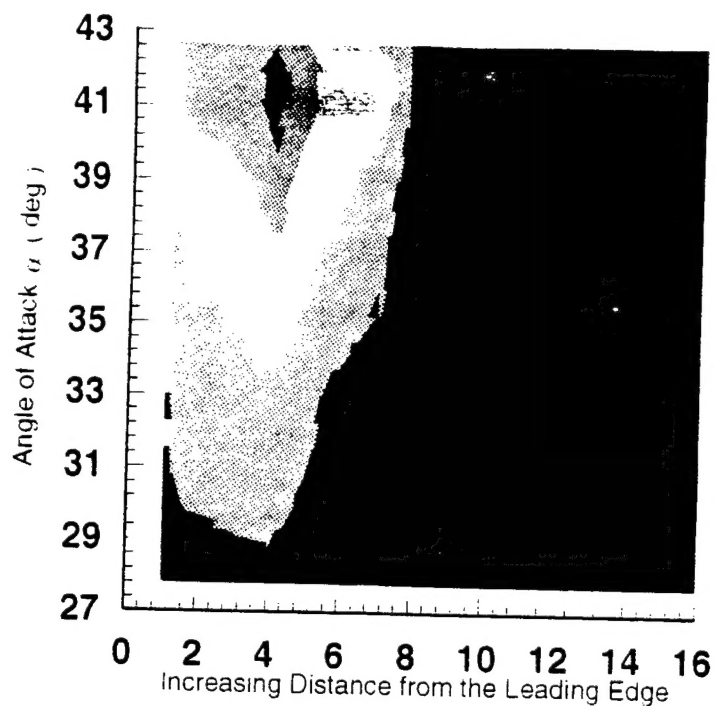
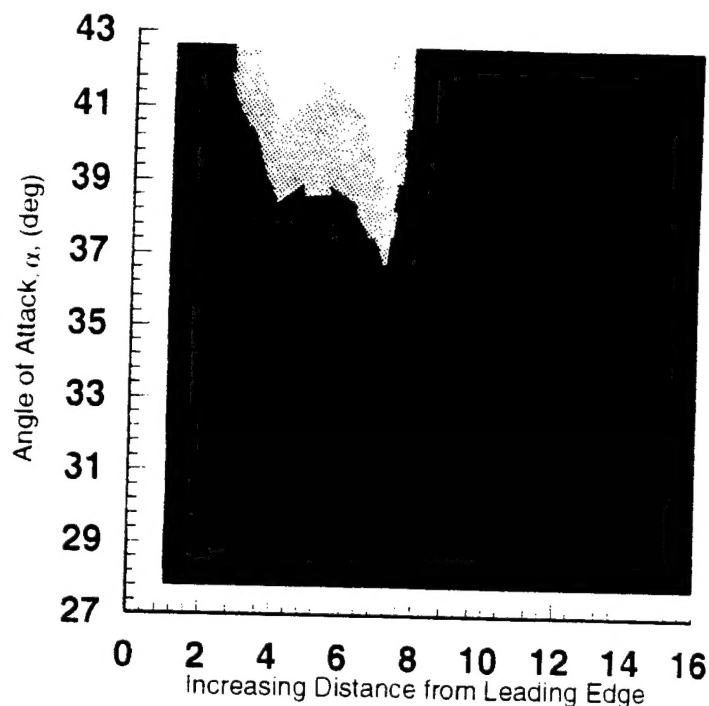


Fig. 11 The fuzzy controller configuration.



(a) Without Flaps



(b) With Flaps

Cp

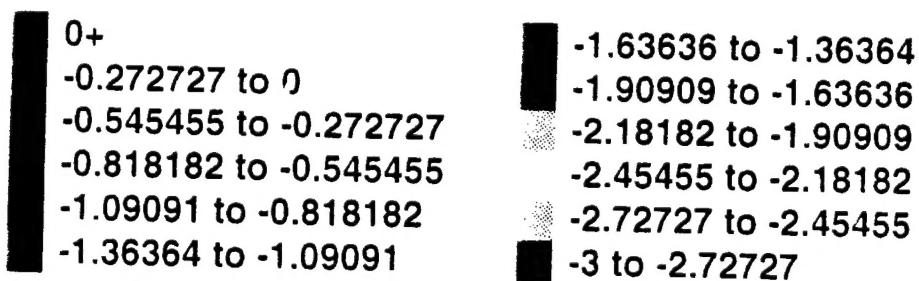


Fig. 12 Surface pressure distribution in a cross-flow plane (upper pressure port raw). Unsteady flow: (a) flaps off (b) flaps on.